

Contract:

ENEA – Banco Interamericano de Desarrollo (BID)/InterAmerican Development Bank (IDB)

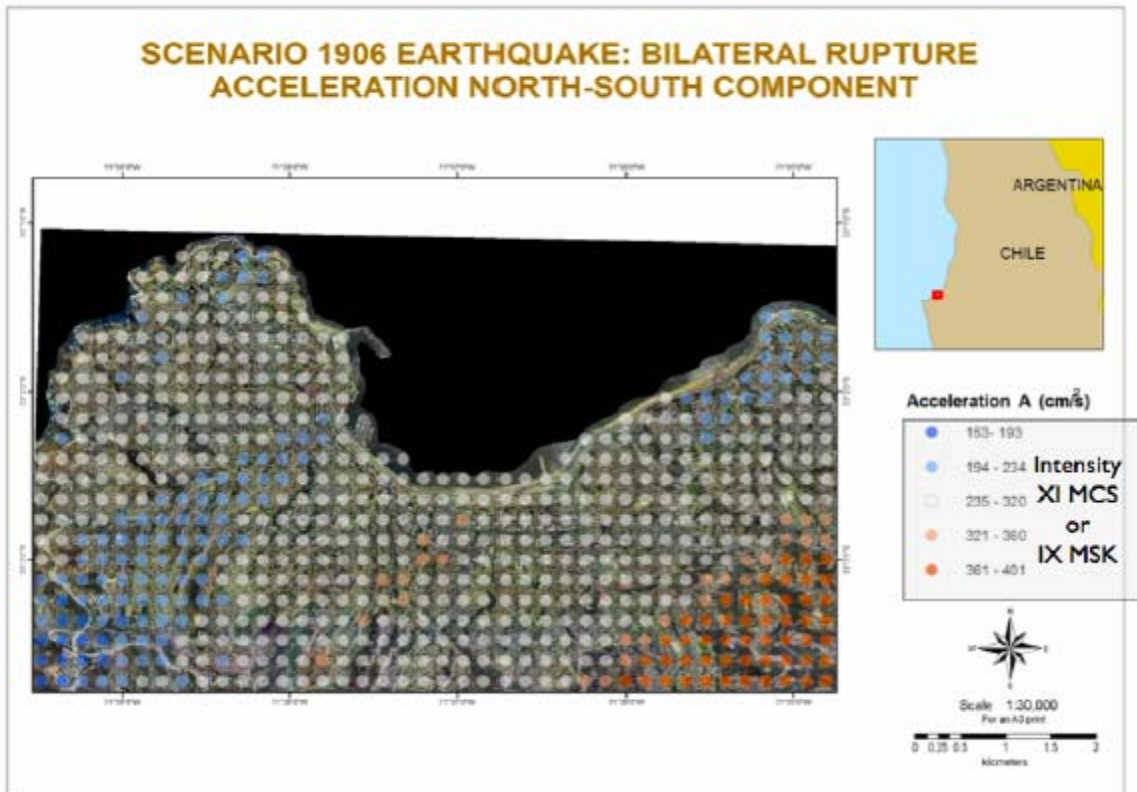
# Manejo de Riesgos en Valparaiso, Servicios Técnicos

Acronym: "MAR VASTO"

ATN/II-9816-CH

Contract n.

PRM.7.035.00-C



## EARTHQUAKE HAZARD IN THE CITY OF VALPARAISO

3			Name				
			Signature				
2			Name				
			Signature				
1			Name				
			Signature				
0	Date	30.06.2008	Name	F. ROMANELLI			
			Signature	<i>F. Romanelli</i>			
				<b>AUTHORS</b>			

## INDEX

Preface	Pag.	3
1. Introduction	Pag.	4
2. Seismic hazard at regional scale	Pag.	6
3. Extended source models	Pag.	10
4. Parametric tests	Pag.	11
4.1 Site at 100km	Pag.	12
4.2 Receiver at 60 km	Pag.	15
4.3 1906 Event at Valparaiso	Pag.	16
4.4 1985 Event at Valparaiso	Pag.	19
4.5 Validation	Pag.	22
5. Seismic input at urban scale	Pag.	25
6. Seismic input along selected profiles: site response estimation	Pag.	29
7. Final remarks	Pag.	38
8. Selected references focusing on the hazard in Valparaiso	Pag.	39
9. References	Pag.	40

## **PREFACE**

The work has been carried out during the *in situ* investigation of the Italian experts, done in the framework of two missions at Valparaíso (May and October-December 2007), with the help of many local Organizations (see General Progress Reports). In particular, we appreciated very much the cooperation of the personnel of the “Oficina de Gestion Patrimonial - OGP” of the Valparaiso Municipality (headed by Paulina Kaplan Depolo) and SHOA (Servicio Hidrografico y Oceanografico de la Armada de Chile).

The work has been fruitfully carried out with the Chilean scientific team, in particular with Prof. R. Saragoni, Prof. M. Astroza (University of Chile, Santiago) and some of their PhD students (e.g. S. Ruiz and T. Sturn) for the Seismic Hazard and with Dr. Dante Gutierrez (SHOA) for the Tsunami Hazard.

This report, regarding WP3 activities (study of seismic hazard), has been carried out by the WP3 leader ICTP.

ICTP Team composition:

Prof. Giuliano Panza	Scientific Coordinator
Hoby Raza	PhD Student
Elisa Zuccolo	PhD Student
Cristina La Mura	PhD Student
Dr. Fabio Romanelli	Senior Researcher
Dr. Franco Vaccari	Senior Researcher

## 1. INTRODUCTION

Strong earthquakes, such as the 1985 Michoacan, the 1995 Kobe, and the recent 2008 Sichuan earthquake, have acted as catalysts for the use of zoning in seismic risk management. Politicians and administrators are more and more interested in the rapid reconstruction according to criteria which reduce the probability of repetition of a disaster. A drastic change is required in the orientation of zoning that must be a predisaster activity performed to mitigate the effects of the next earthquake, using all available technologies. We must be able to take preventive steps, extending, in a scientifically acceptable way, the obtained results to areas in which no direct experience has yet been gained. Seismic zoning can use scientific data banks, integrated in an expert system, by means of which it is possible not only to identify the safest and most suitable areas for urban development, but also to define the seismic input that is going to affect a given building. Seismic hazard assessment, necessary to design earthquake-resistant structures, can be performed in various ways, following a probabilistic or a deterministic approach. National seismic codes and zonations are often based on seismic hazard assessments computed with a probabilistic analysis (e.g. Cornell, 1968; SSHAC, 1997, Gshap; Tanner and Shedlock, 2004).

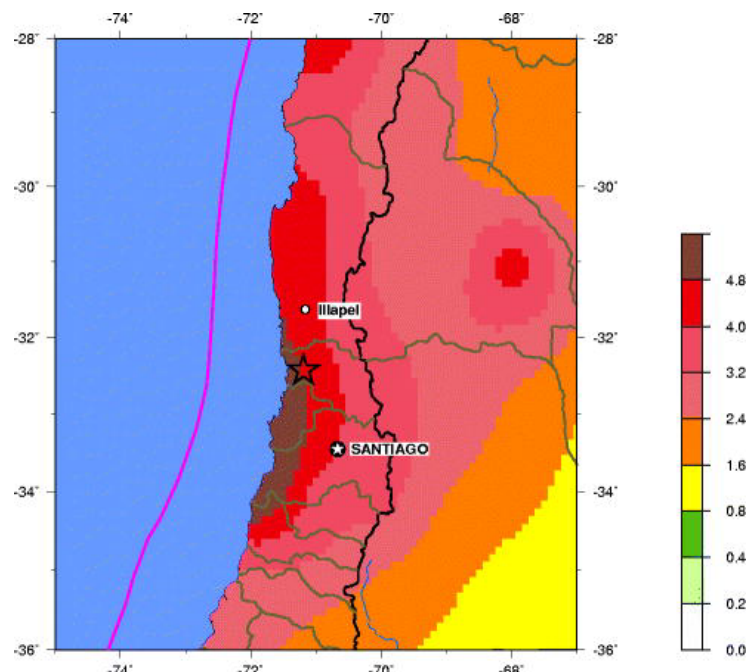


Figure 1: Seismic hazard map (PGA in  $m/s^2$  with 10% probability of exceedence in 50 years) of the Central part of Chile (source: [http://neic.usgs.gov/neis/bulletin/neic\\_tibx\\_w.html](http://neic.usgs.gov/neis/bulletin/neic_tibx_w.html)) using the traditional probabilistic approach (see <http://www.seismo.ethz.ch/gshap/>)

Nevertheless, the probabilistic method is not sufficiently reliable to completely characterise the seismic hazard because of the difficulty to define the seismogenic zones and to evaluate correctly the occurrence of the earthquakes (frequency–magnitude relations) and the propagation of their effects (attenuation laws). Moreover, the mathematical model of probabilistic seismic hazard analysis is often inaccurate and introduces systematic errors in the calculation process that leads to results that could represent only a gross approximation of the reality (Klügel, 2007). A more adequate description of the seismic ground motion can be done following a neo-deterministic approach, which allows to give a realistic description of the seismic ground motion due to an earthquake of given distance and magnitude (e.g. Panza et al., 2001). The approach is based on modelling techniques that have been developed from the knowledge of the seismic source generation and propagation processes. It is very useful because it permits to define a set of earthquake scenarios and to compute the associated synthetic signals, without having to wait for a strong event to occur.

Synthetic signals can be produced in short time and at a very low cost/benefit ratio, and can be used as seismic input in subsequent engineering analysis aimed at the computation of the seismic response of the structures. Modelling can be done at different level of detail, depending on the available knowledge of geological, geophysical, seismological and seismotectonical setting. The realistic modelling of the ground motion is a very important base of knowledge for the preparation of groundshaking scenarios that represent a valid and economic tool to be fruitfully used by civil engineers, supplying a particularly powerful tool for the prevention aspects of Civil Defense. Where the numerical modelling is successfully compared with records (as in the case of the Valparaiso, 1985 earthquake), the synthetic seismograms permit the generation of groundshaking maps, based upon a set of possible scenario earthquakes. Where no recordings are available for the scenario event, the synthetic signals can be used to estimate the ground motion without having to wait for a strong earthquake to occur (pre-disaster microzonation).

The major goal of the WP is to provide a dataset of synthetic time series representative of the potential ground motion at the bedrock of Valparaiso, especially at selected sites (e.g. the three important churches located in the Valparaiso urban area: La Matriz, San Francisco, Las Hermanitas de la Providencia), for different scenarios; the characteristics of the calculated signals (e.g. amplitude, frequency content and duration of shaking) are determined by the earthquake source process and the wave propagation effects of the path between the source and the site. The generation and selection of realistic time series for design is essentially a problem of choosing appropriately from among a number of future earthquake scenarios, whose most important characteristics are their magnitude and the distance to the site. From hazard maps it is possible to define the scenario earthquakes to be used in planning exercises and earthquake engineering studies. Such an analysis is accomplished by hazard deaggregation, in which the contributions of individual earthquakes to the total seismic hazard, their probability of occurrence and the severity of the ground motions are ranked in the order. Using the individual components ("deaggregating" the events driving the hazard at the target region) of these hazard maps, the user can properly select the appropriate scenarios given their location, regional extent, and specific planning requirements. Thus, the definition of earthquake scenarios depends on many factors (e.g. historical seismicity, seismotectonic studies, engineering considerations) and it has not to be intended as an earthquake prediction. That is, no one knows in advance when or how large a future earthquake will be, but making assumptions about the size and location of a hypothetical future earthquake, one can make a reasonable prediction of the *effects* (e.g. groundshaking) for planning and preparedness purposes. Intermediate-term middle-range earthquake prediction is possible at different scales (e.g. Peresan et al., 2005).

One of the most difficult tasks in earthquake scenario modeling is the treatment of uncertainties since each of the key parameters has an uncertainty and natural variability, which often are not quantified explicitly. A possible way to handle this problem is to vary the modeling parameters systematically. Actually, a severe underestimation of the hazard could come by fixing a priori some source characteristics and thus the parametric study should take into account the effects of the various focal mechanism parameters (i.e. strike, dip, rake, depth etc.). The analysis of the parametric studies will allow to generate advanced groundshaking scenarios for the proper evaluation of the site-specific seismic hazard, with a complementary check based on both probabilistic and empirical procedures. Once the gross features of the seismic hazard are defined, and the parametric analyses have been performed, a more detailed modelling of the ground motion can be carried out for sites of specific interest. Such a detailed analysis should take into account the source characteristics, the path and the local geological and geotechnical conditions. This deterministic modelling goes well beyond the conventional deterministic approach taken in hazard analyses - in which only a simple wave attenuation relation is invoked - in that it includes full waveform modelling.

## 2. SEISMIC HAZARD AT A REGIONAL SCALE

The procedure for the neo-deterministic seismic zoning (e.g. Panza et al., 1996; Panza et al., 2001) represents one of the new and most advanced approaches and it has been applied successfully to many areas spread worldwide (e.g. Parvez et al., 2003). It can be used also as a starting point for the development of an integrated approach that will combine the advantages of the probabilistic and deterministic methods, thus minimizing their respective drawbacks. This approach addresses some issues largely neglected in probabilistic hazard analysis, namely how crustal properties affect attenuation: ground motion parameters are not derived from overly simplified attenuation functions, but rather from synthetic time histories. Starting from the available information on the Earth's structure, seismic sources, and the level of seismicity of the investigated area, it is possible to estimate peak ground acceleration, velocity, and displacement (PGA, PGV, and PGD) or any other parameter relevant to seismic engineering, which can be extracted from the computed theoretical signals. This procedure allows us to obtain a realistic estimate of the seismic hazard in those areas for which scarce (or no) historical or instrumental information is available and to perform the relevant parametric analyses.

Synthetic seismograms can be constructed to model ground motion at sites of interest, using knowledge of the physical process of earthquake generation and wave propagation in realistic media. The signals are efficiently generated by the modal summation technique (e.g. Panza and Suhadolc, 1987; Panza et al., 2001), so it becomes possible to perform detailed parametric analyses at reasonable costs. The flowchart of the procedure is shown in Figure 2. The first problem to tackle in the definition of seismic sources is the handling of seismicity data. Basically, what is needed is an evenly spaced distribution of the maximum magnitude over the territory, but the data available from earthquake catalogues are widely scattered. Furthermore, earthquake catalogues are both incomplete and affected by errors, so a smoothed distribution is preferable (Panza et al., 2001).

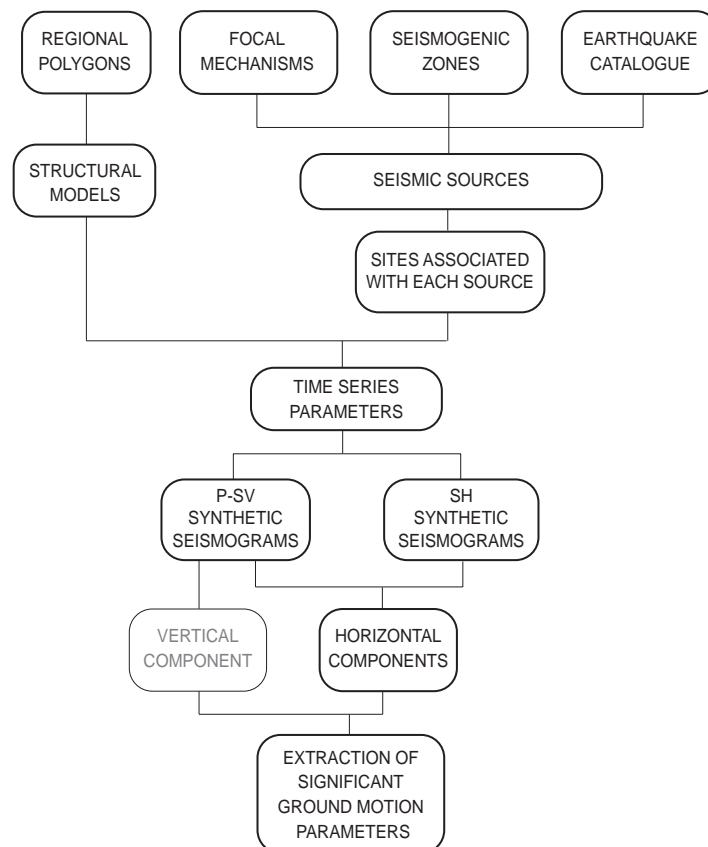
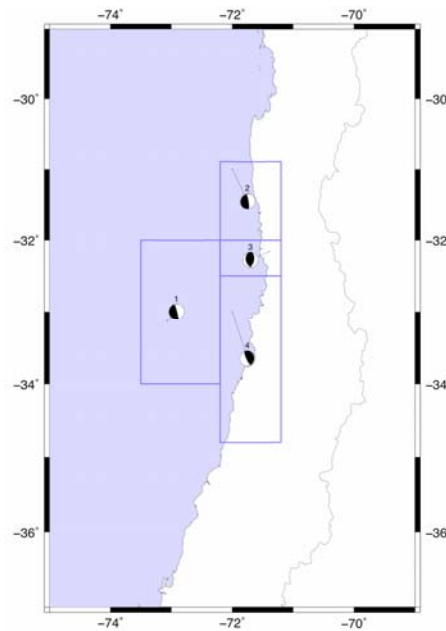


Figure 2: flow-chart of the neo-deterministic procedure for seismic hazard assessment at regional scale (see Panza et al., 2001). The vertical component is routinely not used.

Specifically seismograms are computed at the nodes of a grid with step  $0.2^\circ$ , that covers the region of the Central Chile territory. 107 events have been selected from the dataset collected by the Servicio Sismologico Universidad de Chile (<http://ssn.dgf.uchile.cl/home/terrem.html>), that have been considered as the most representative between the destructive earthquakes occurred in Chile, from 1570 till present, with a magnitude greater than 7. Four different seismogenic zones have been defined, using the information about the seismicity and tectonics of the area; the seismicity is discretized into  $0.2^\circ \times 0.2^\circ$  cells, assigning to each cell the maximum magnitude recorded within it; a smoothing procedure is then applied to account for spatial uncertainty and for source dimensions. Since the aim of this step is the average regional definition of seismic input, a double-couple point source, with a focal mechanism consistent with the regime of the pertinent seismogenic zone (e.g. Panza et al., 2001), as shown in Figure 3.



	date	mag	strike	dip	rake
Zone 1	16/10/1981	7.2	345	86	-93
Zone 2	28/03/1965	7.3	350	80	-100
Zone 3	06/07/1979	6.0	11	54	105
Zone 4	16/08/1906	8.2	3	15	117

Figure 3: Seismogenic zones and their representative events

To define the physical properties of the source-site paths, the territory is characterized by a structural model composed of flat, parallel anelastic layers that represent the average lithosphere properties at a regional scale. We have defined the regional bedrock structural model (the uppermost layers are shown in Table 1) starting from the model proposed by Mendoza et al. (1994) and the related references.

Thickness(km)	Density(g/cm <sup>3</sup> )	Vp(km/s)	Vs(km/s)	Qp	Qs
1.0000	1.70	4.000000	2.310000	100.00	50.00
3.0000	2.00	4.750000	2.740000	200.00	100.00
4.0000	2.30	5.560000	3.210000	400.00	200.00
8.9000	2.50	6.070000	3.500000	500.00	250.00
5.5000	2.65	6.530000	3.770000	600.00	300.00
15.000	2.80	7.000000	4.040000	600.00	300.00
30.000	3.28	8.000000	4.500000	600.00	300.00

The seismograms have been computed for an upper frequency content of 10 Hz and the point sources are scaled for their dimensions (Size Scaled Point Source) using the relatively simple spectral scaling laws by Gusev (1983). Such a simple source model gives a reliable upperbound of the PGA and, at the same time, permits a realistic estimate of the PGD and PGV. In the following figures, only some examples of the wide set of results are shown.

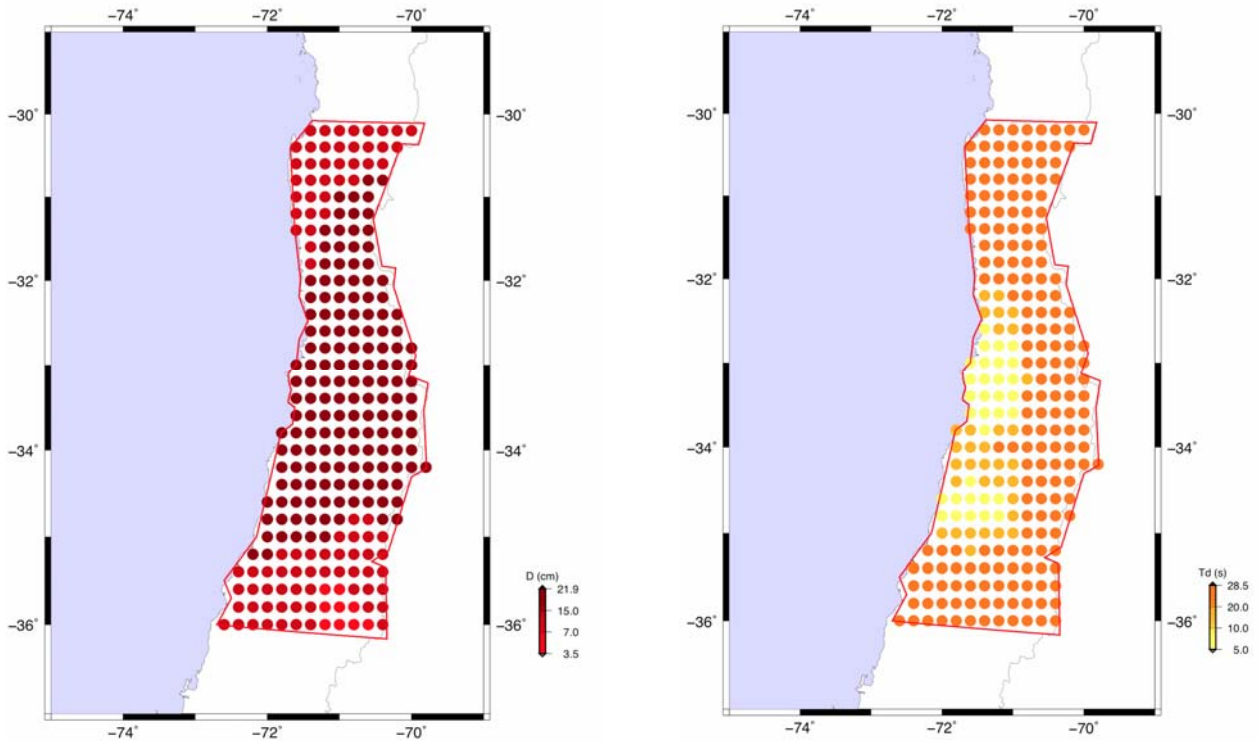


Figure 4: Horizontal PGD distribution and Period in seconds of its maximum

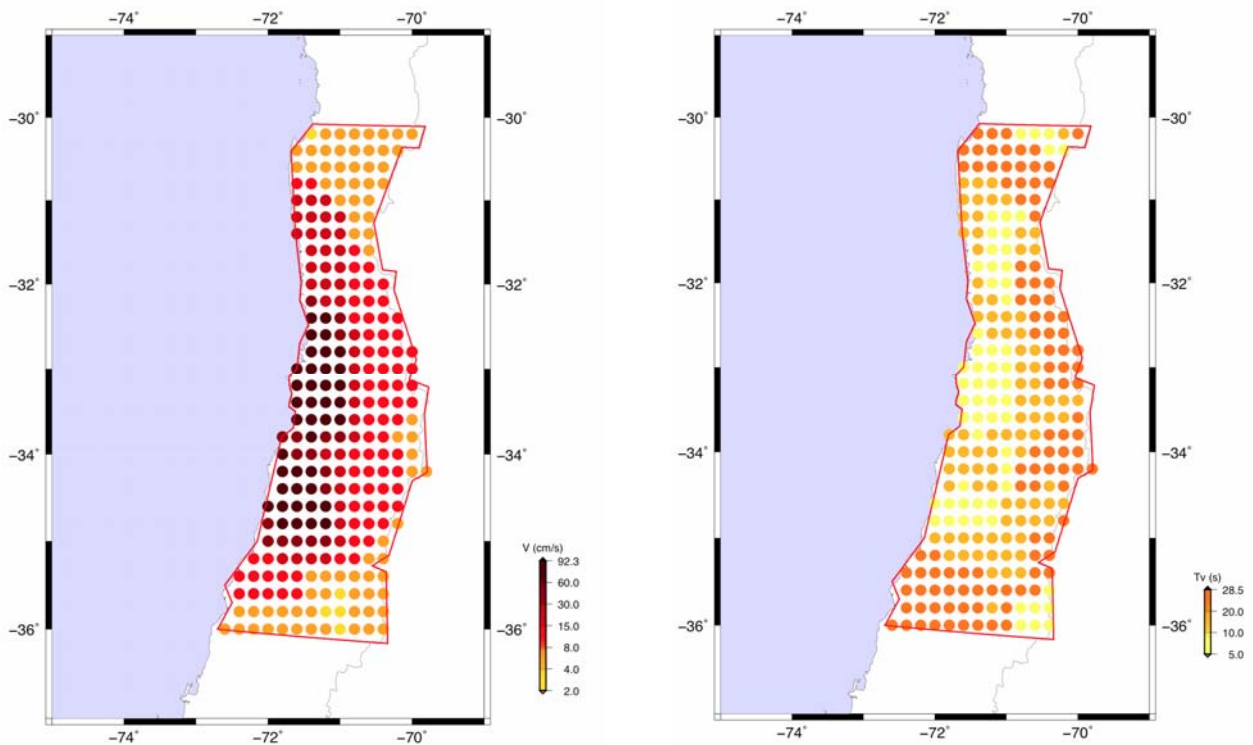


Figure 5: Horizontal PGV distribution and Period in seconds of its maximum.



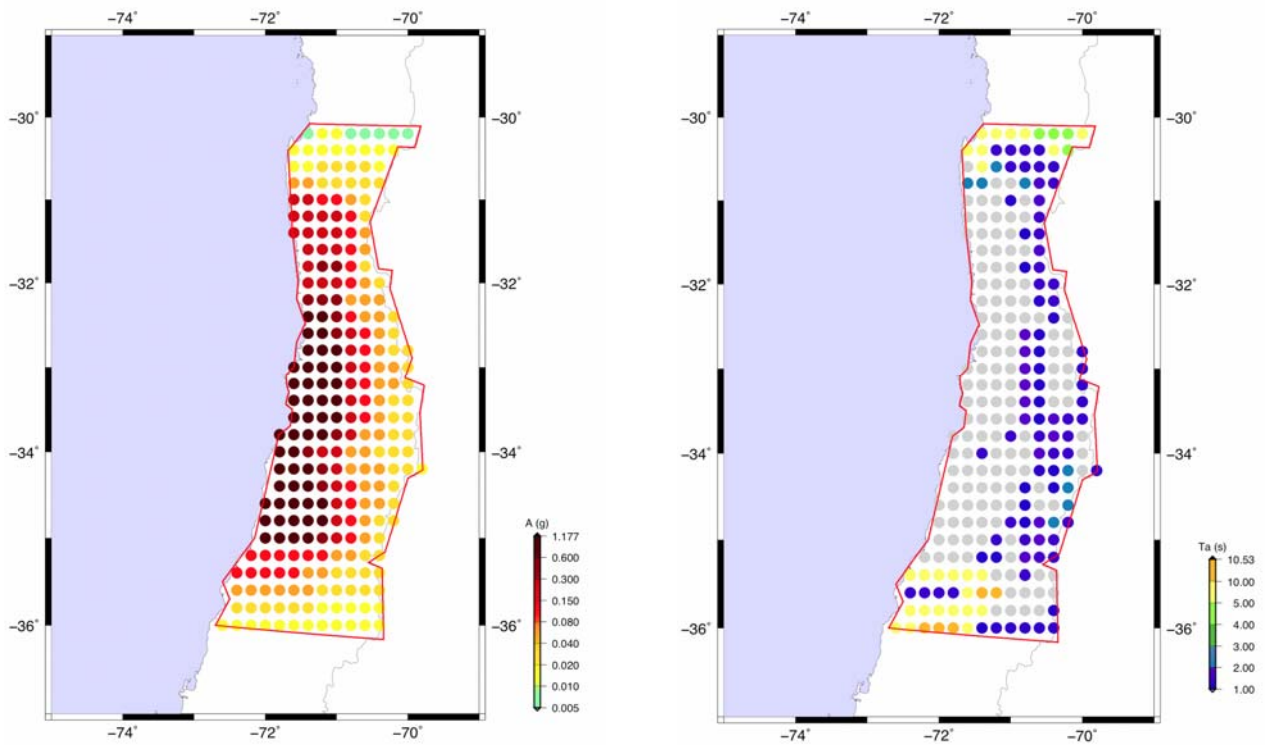


Figure 6: Horizontal PGA distribution and Period in seconds of its maximum

Then, we focused (deaggregating the hazard) on the two most important earthquake scenarios for Valparaíso: the 1985 and 1906 events, belonging to the seismogenic zone 4. These events have been chosen, not only because of their large magnitude, but also because of the damage that they generated in Valparaíso (e.g. Saragoni, 2006).

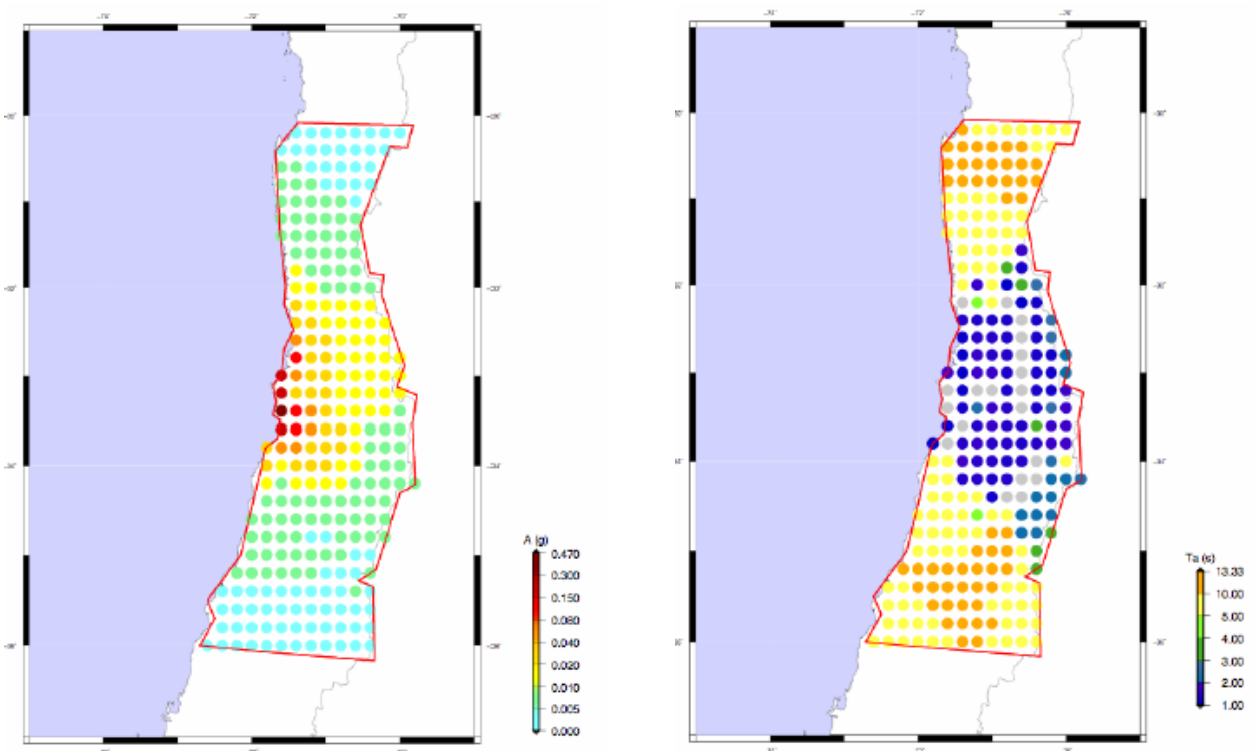


Figure 7: Horizontal PGA distribution and Period in seconds of its maximum after deaggregation

We use the simple model of source (SSPS) to define the upper bound of PGA for the entire study region, that turns out to be about 1.2 g, or 0.5g (after deaggregation), in good agreement with the Intensities values reported for the 1906 event (e.g. Saragoni, 2006; Astroza, 2006). The use of microzonation, considering more complex and realistic sources, allows us to better delimit the zones at a urban scale where the largest PGA can be expected. Therefore our procedure consists in, (a) expeditious and low-cost determination of hazard using simple and easily available information about seismic sources and surrounding medium (this Section), (b) more realistic modeling (next Sections) focussed on items of special interest for which more expensive procedures are necessary and fully justified by the exposed value.

### 3. EXTENDED SOURCE MODELS

In a further step towards realism, to consider the rupture process at the source and the related directivity effect (i.e. the dependence of the radiation at a site on its azimuth with respect to the rupture propagation direction), extended source models have been considered, using the algorithm for the simulation of the source radiation from a fault of finite dimensions, named PULSYN (PULse-based wideband SYNthesis), developed by Gusev and Pavlov (2006). The seismic waves due to an extended source are obtained by approximating it with a rectangular plane surface, corresponding to the fault plane on which the main rupture process is assumed to occur. Effects of directivity and of the energy release on the fault can be easily modeled, simulating the wide-band radiation process from a finite earthquake source/fault. To represent an extended source PULSYN uses the main features of the Haskell (1964) model and discretizes the rectangular fault plane with a grid of point sub-sources. The arrival of the rupture front at a sub source switches its slip. However, unlike Haskell model, the spatial distribution of slip and the rupture velocity are treated as a random process and characterized in a stochastic manner. In fact, the small-scale details of the rupture process, connected to heterogeneities in the stress distribution and, in general, too complicated to be exactly characterized, generate high frequency waves when reached by the rupture front. In this way the code PULSYN generates a source (phase and amplitude) spectrum, which is close in amplitude to the Gusev's (1983) empirical curves and reproduces the directivity (see Figure 8) effects as in the theoretical Haskell model.

With this approach we can simulate the time histories using a (1) Extended Source (ES) and (2) Space and Time Scaled Point Source (STSPS). In the ES case, the source is represented as a grid of point subsources, and their seismic moment rate functions are generated considering each of them as realizations (sample functions) of a non-stationary random process. Specifying in a realistic way the source length and width, as well as the rupture velocity, one can obtain realistic source time functions, valid in the far-field approximation. Finally, to calculate the ground motion at a site, Green functions are computed with the highly efficient and accurate modal summation technique, for each subsource-site pair, and then convolved with the subsource time functions and, at last, summed over all subsources. Furthermore, assuming a realistic kinematic description of the rupture process, the stochastic structure of the accelerograms can be reproduced, including the general envelope shape and peak factors. The extended seismic source model allows us to generate a spectrum (amplitude and phase) of the source time function that takes into accounts both the rupture process and directivity effects, also in the Near Source region. In the second case (STSPS), we use a mixture of extended and point sources. We sum up the source time functions generated by the distributed (point) subsources in order to consider obtain the equivalent single source, representative of the entire space and time structure of the extended source, and the related Green Function. In such a way it is possible to perform expeditious parametric studies, useful for engineering analysis (e.g. Zuccolo et al., 2008) to, investigate the dependence of the ground motion (in the time and frequency domain) on source parameters (geometry, energy release etc.).

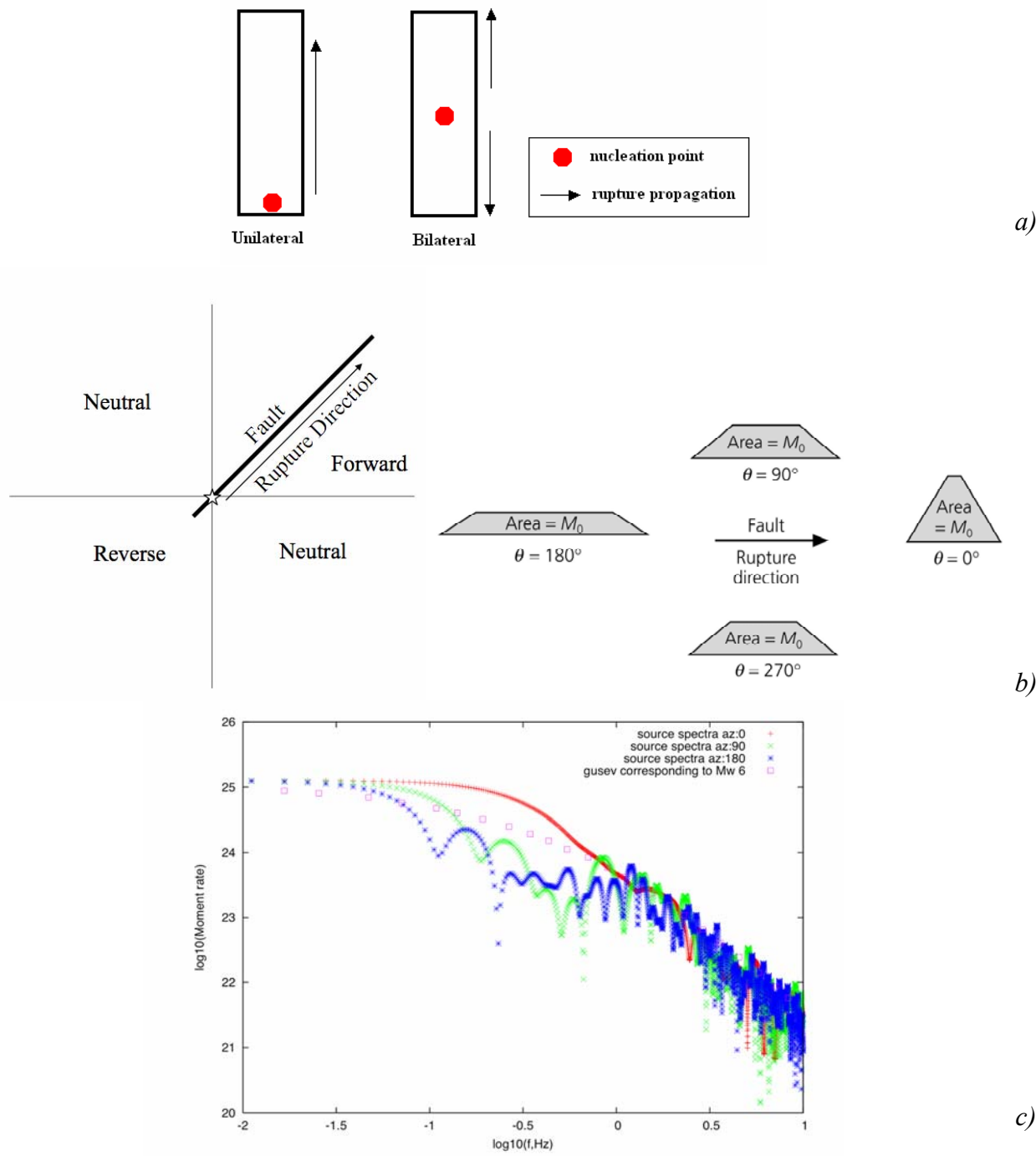


Figure 8: a) Unilateral and Bilateral rupture processes, b) directivity effect and c) an example of source spectra for a unilateral rupture at three different sites (forward, neutral and reverse)

#### 4. PARAMETRIC TESTS

The synthetic signals database described in Section 2 has been greatly expanded by performing a parametric study of the ground motion, taking into account the variations due to the choice of the focal mechanism parameters. Varying the geometry of the seismic source, different ground motions at the Valparaiso site have been studied, in order to consider maximum excitation in both longitudinal (P-SV motion) and transverse (SH motion) direction, and in order to consider (starting from the Maximum Historical Earthquake) both the Maximum Credible Earthquake and the Maximum Design Earthquake.

The computation of synthetic seismograms (displacements, velocities and accelerations for the radial, transverse and vertical components) has been carried out with a cut-off frequency of 10 Hz.

All the focal mechanism parameters of the original source models obtained from the seismic catalogues (see also Section 2) have been varied in order to find the source mechanism producing the maximum amplitude of the various ground motion components. The preliminary parametric test has been performed to estimate the dependence of the radiation pattern on the orientation of the fault plane. This kind of analysis has the purpose to allow for limited changes in the assumed strike-receiver angle (that is uniquely determined by the strike of the fault and the coordinates of the epicentre and the receiver) to avoid the case when one of the three components of motion corresponds to a minimum of radiation. See Figure 9 for an explanation of the conventions adopted.

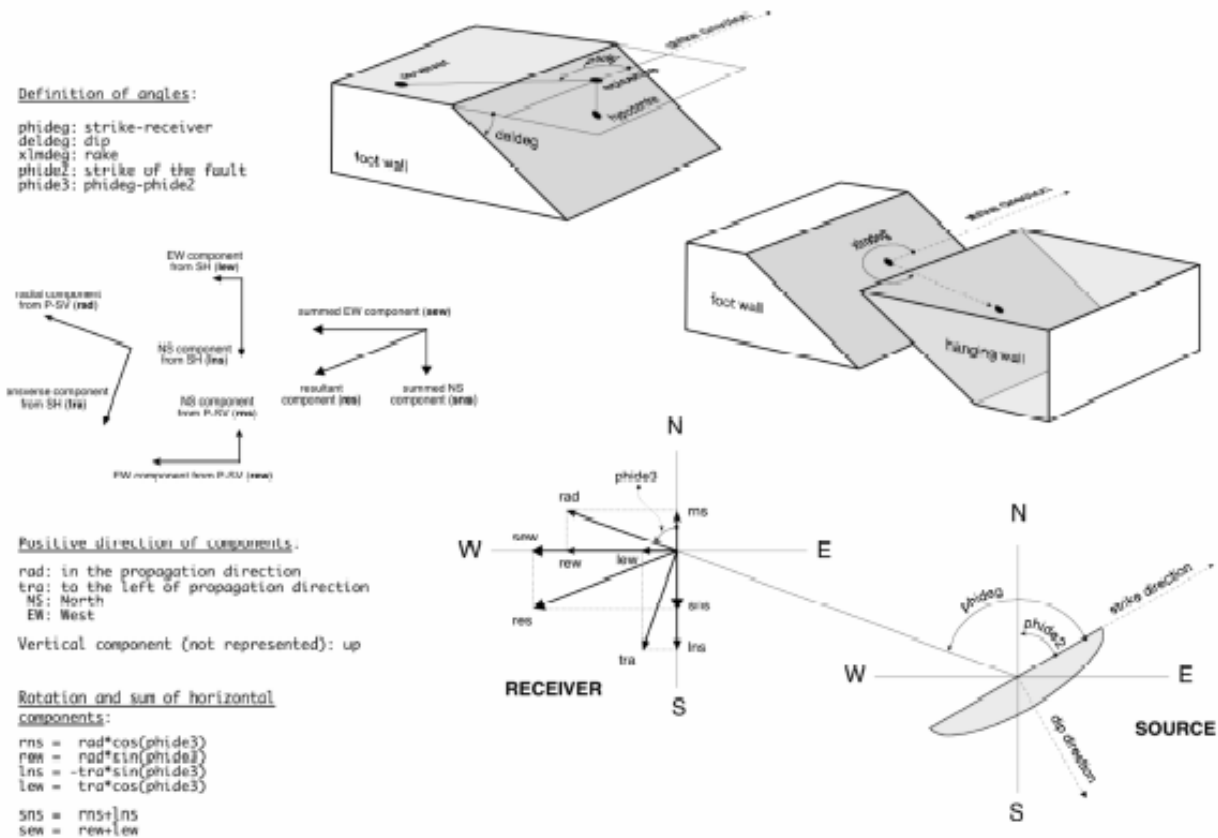


Figure 9: seismic source parameters and conventions adopted in this report.

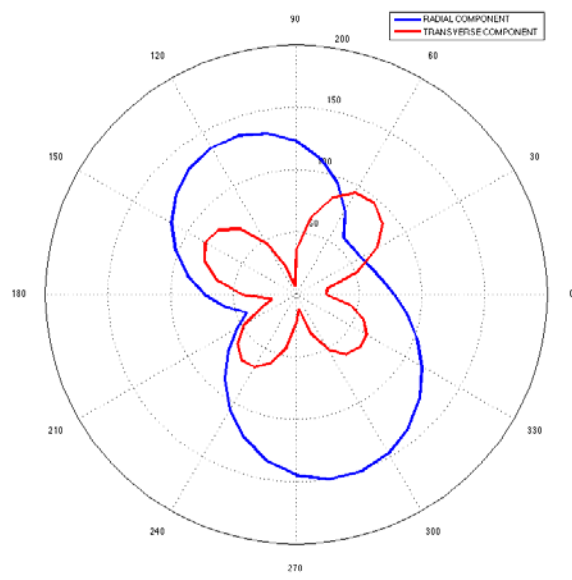
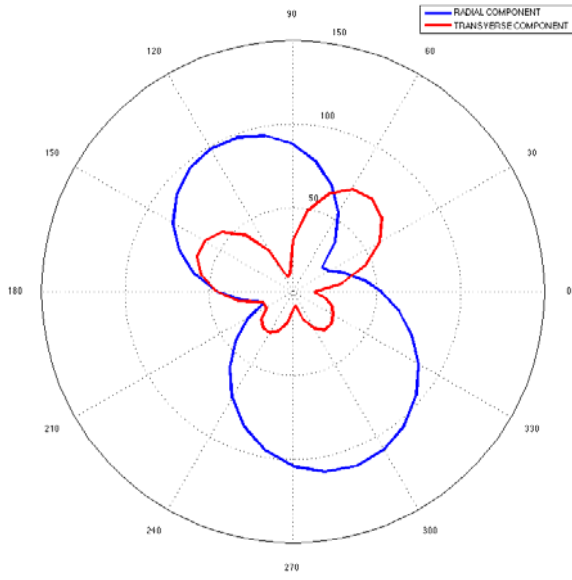
#### 4.1 SITE AT 100KM

The hypothetical receiver is supposed to be at an epicentral distance of 100 km; two focal mechanisms are adopted as starting models: the one proposed by Choy and Dewey (1988), with a strike of  $360^\circ$ , a dip  $35^\circ$ , a rake of  $105^\circ$  and the result given by the CMT Catalogue of Harvard (<http://www.globalcmt.org/>). In the next figures, examples of the results of the parametric studies that have been performed changing the strike-receiver ( $\phi$ ), keeping fixed the dip ( $\delta$ ), rake ( $\lambda$ ) and the hypocentral depth ( $h$ ), are shown for SSPS and STSPS.

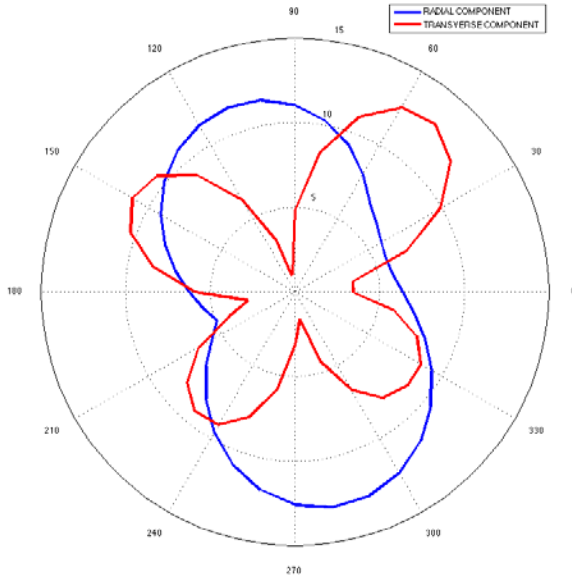
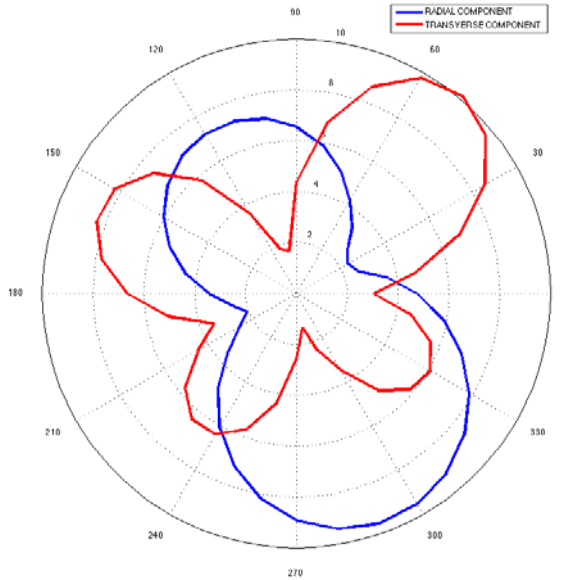
**CMT ( $\delta=25^\circ, \lambda=110^\circ, h=25\text{km}$ )**

**CHOY ( $\delta=35^\circ, \lambda=105^\circ, h=29\text{km}$ )**

a)



b)



c)

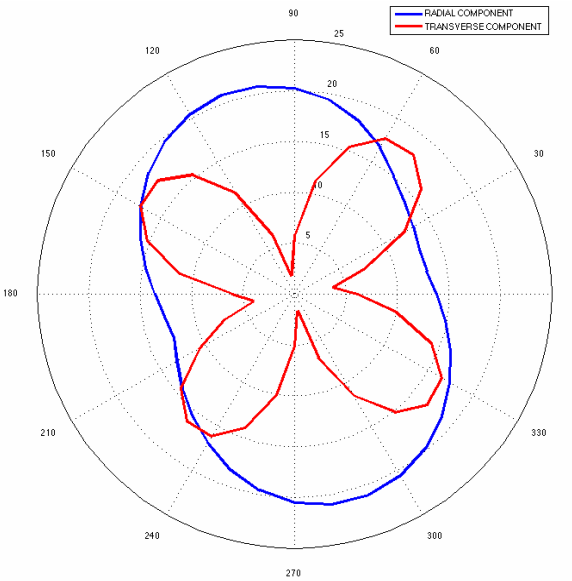
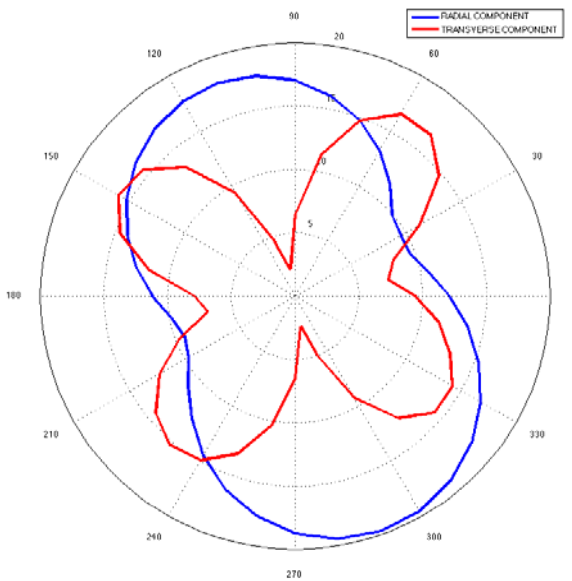
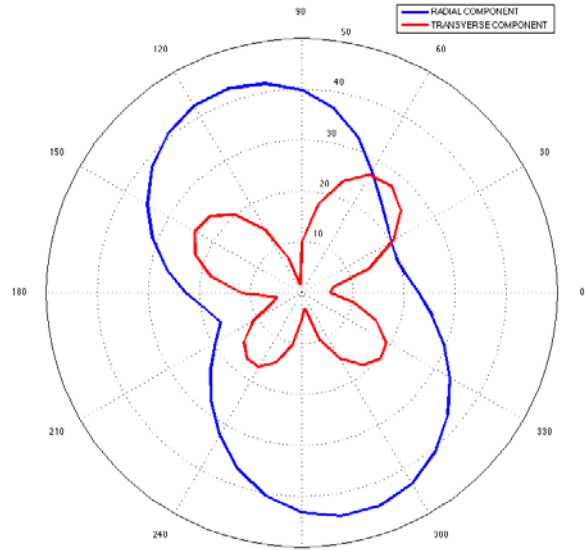
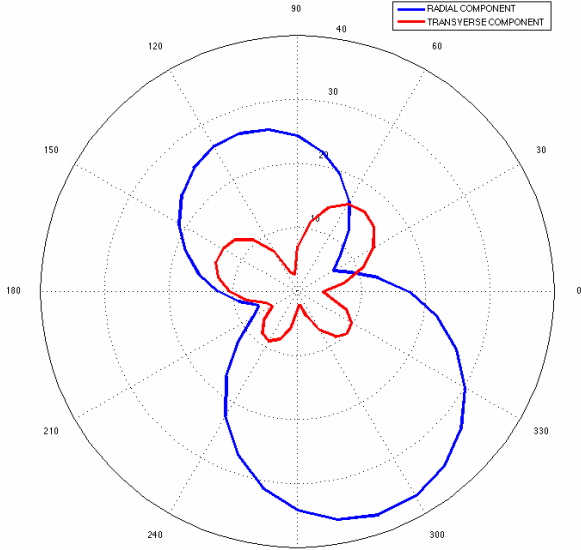


Figure 10: a) PGA, b) PGV, c) PGD variation with strike-receiver; SSPS.

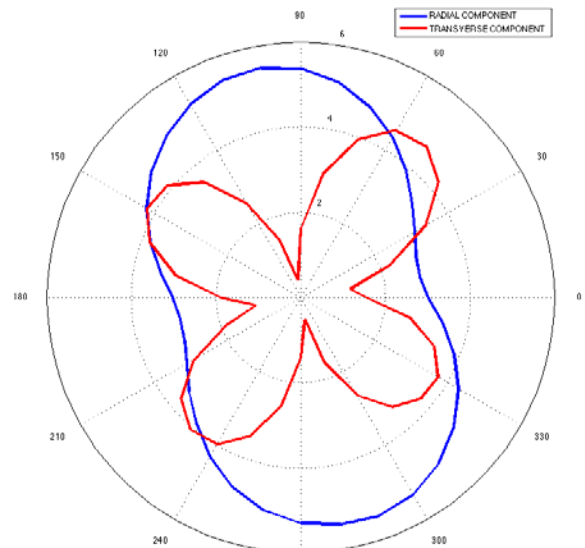
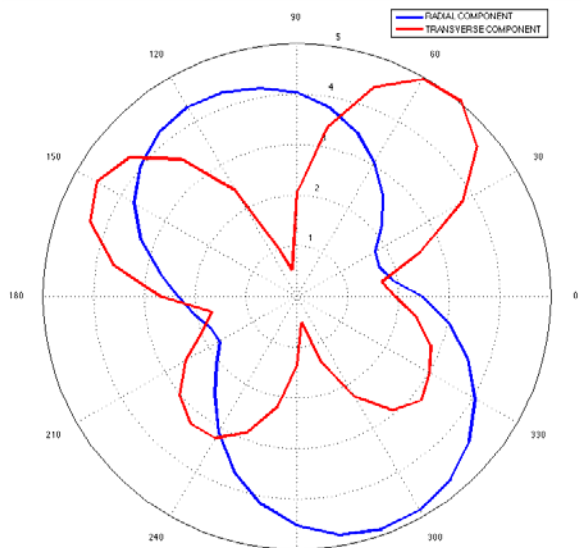
**CMT ( $\delta=25^\circ, \lambda=110^\circ, \text{depth}=25\text{km}$ )**

**CHOY ( $\delta=35^\circ, \lambda=105^\circ, \text{depth}=29\text{km}$ )**

a)



b)



c)

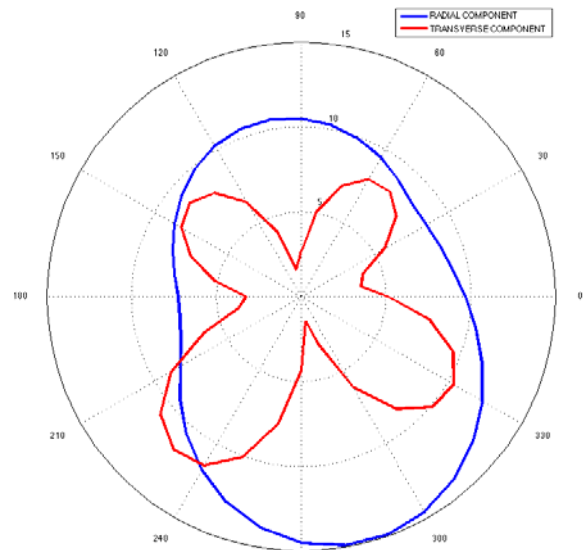
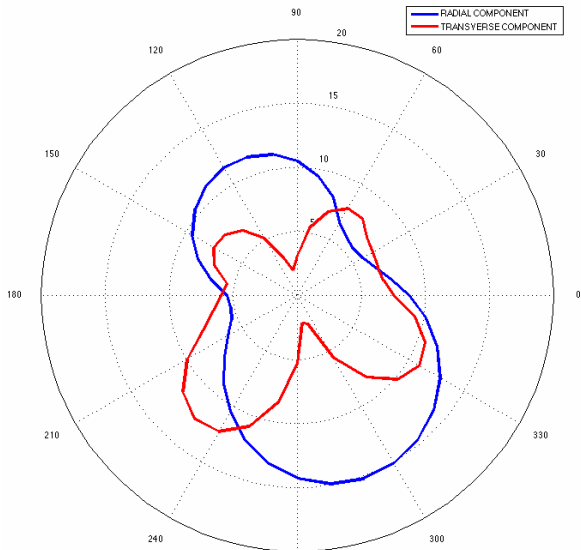


Figure 11: a) PGA, b) PGV, c) PGD variation with strike-receiver; STSPS.

## 4.2 RECEIVER AT 60 KM

The hypothetical receiver is supposed to be at an epicentral distance of 60 km; one focal mechanism is adopted as starting model:

the one given by the CMT Catalogue of Harvard (<http://www.globalcmt.org/>) but with depth 25km. In the next figures, examples of the results of the parametric studies that have been performed changing the strike-receiver are shown.

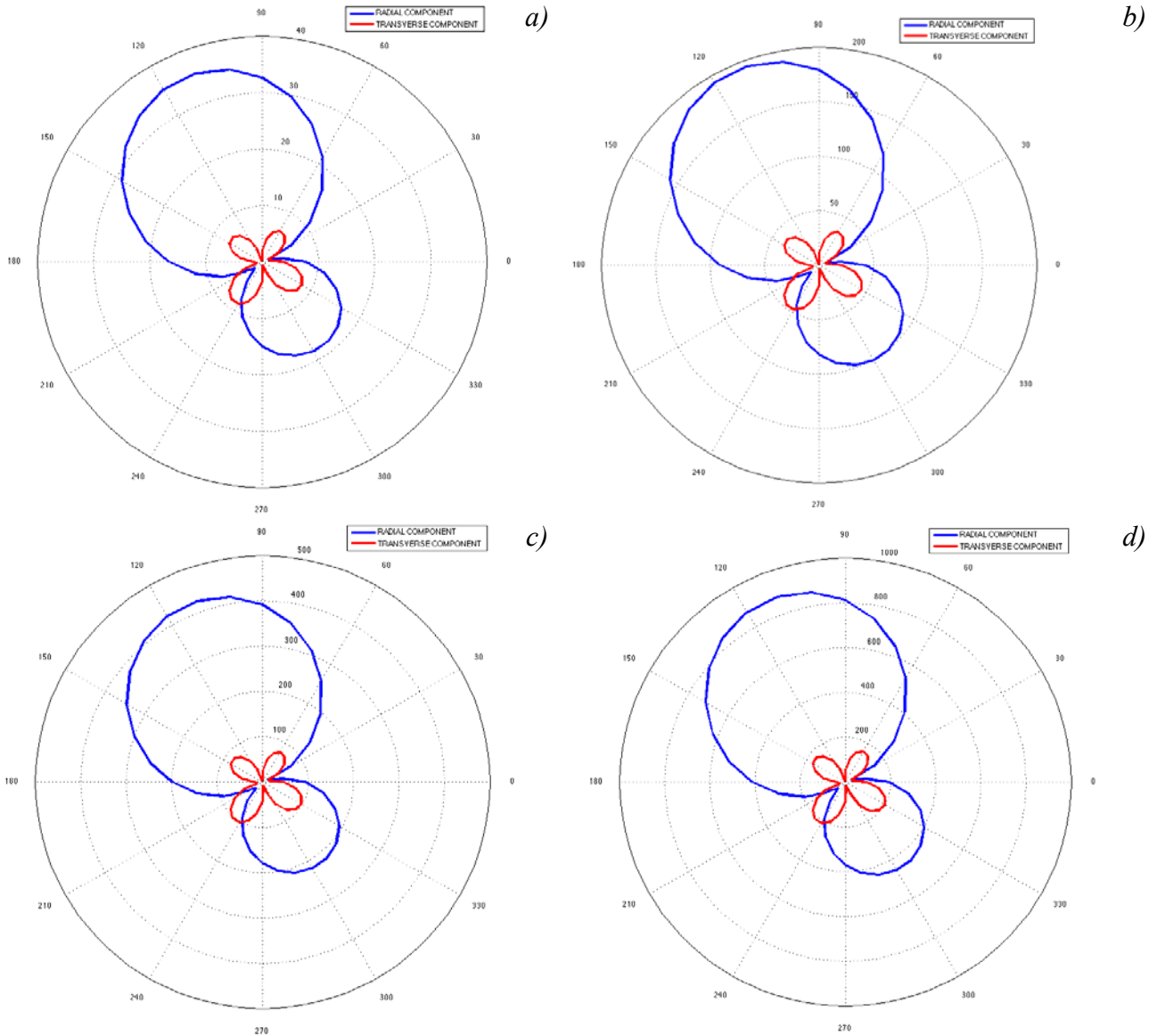


Figure 12: PGA variation with strike-receiver for magnitude 6, 7, 7.5 and 8; SSPS.

### 4.3 1906 EVENT AT VALPARAISO

The receiver is supposed to be in the Valparaiso urban area, at an epicentral distance of about 48 km. In the next figures, examples of the results of the parametric studies that have been performed changing the strike-receiver ( $\phi$ ), the dip ( $\delta$ ), the rake ( $\lambda$ ) angles, the hypocentral depth ( $h$ ), and directivity condition, are shown for SSPS and STSPS.

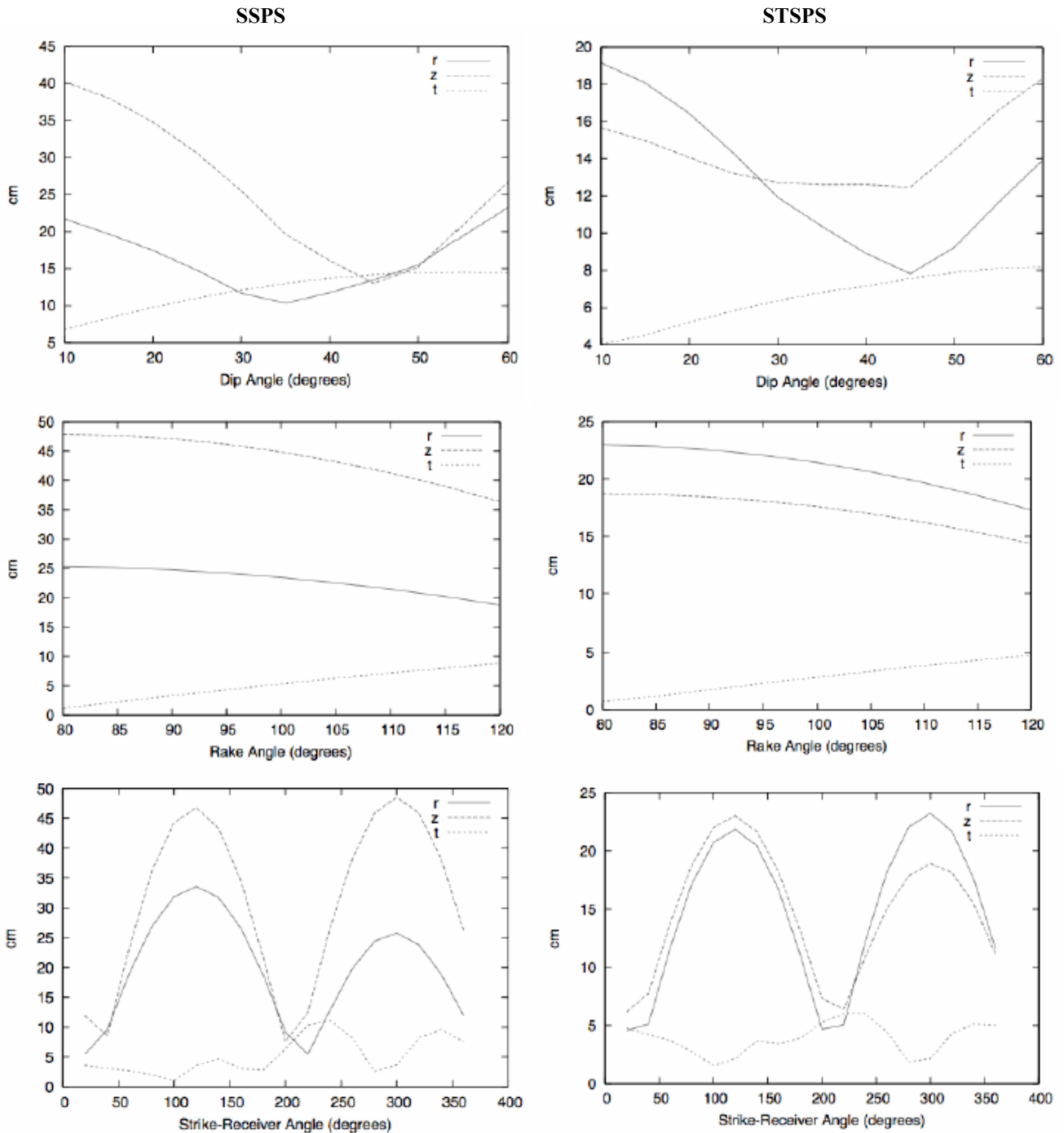


Figure 13: Variation of PGD (cm) with strike, dip and rake for the three components of motion (radial, transverse and vertical); SPSS and STSPS.



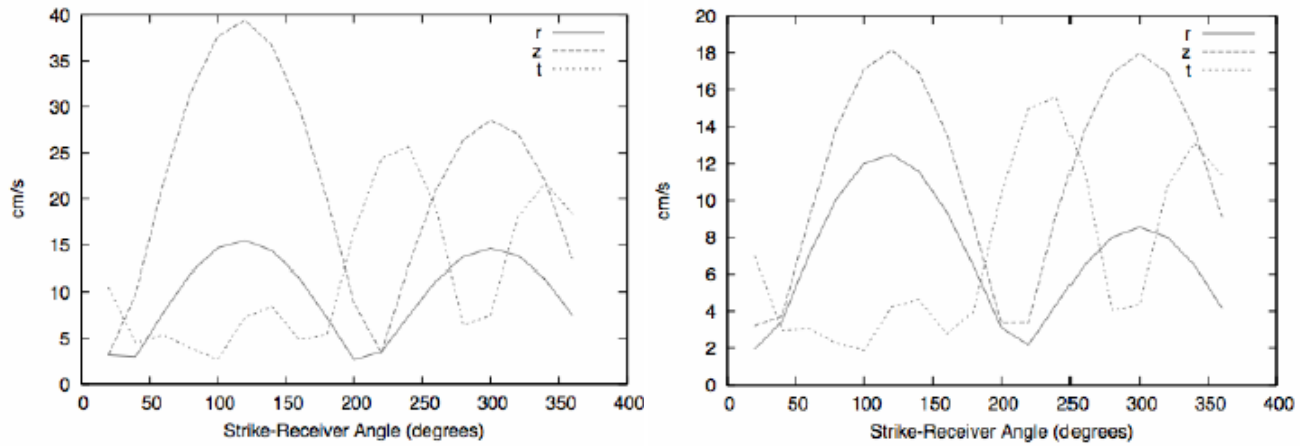


Figure 14: Variation of PGV (cm) with strike for the three components of motion (radial, transverse and vertical); SPSS and STSPS

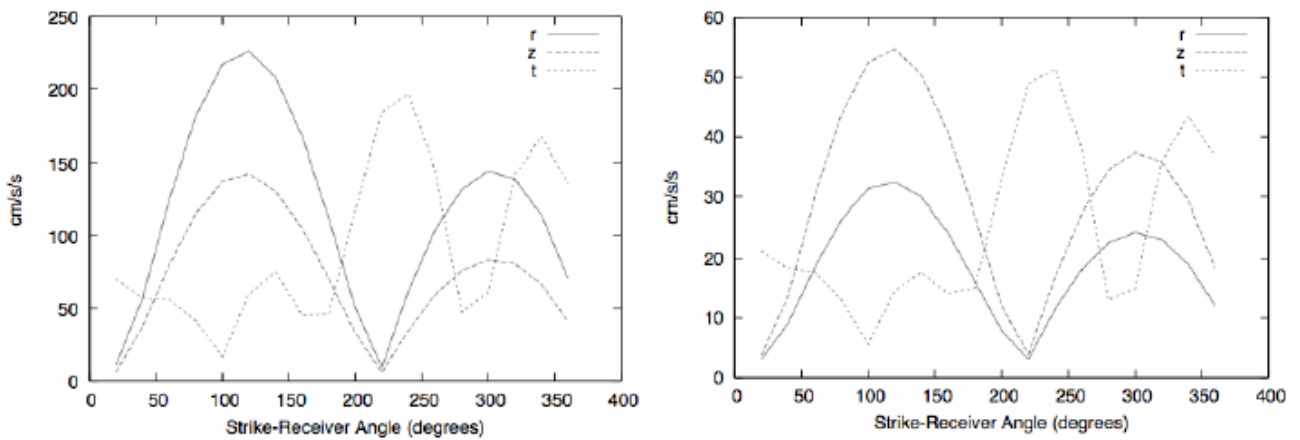


Figure 15: Variation of PGA (cm) with strike for the three components of motion (radial, transverse and vertical); SPSS and STSPS

The results of these parametric studies allow us to fix some of the focal mechanism parameters that will be used in Section 6 for the computation of synthetic signals along detailed profiles for this scenario earthquake: the same values of dip and rake (respectively 15 and 105°) will be adopted, but for the strike receiver, we will use, respectively for transverse and radial component of motion, 230° and 300°, values corresponding to the maximum ground motion amplitude.

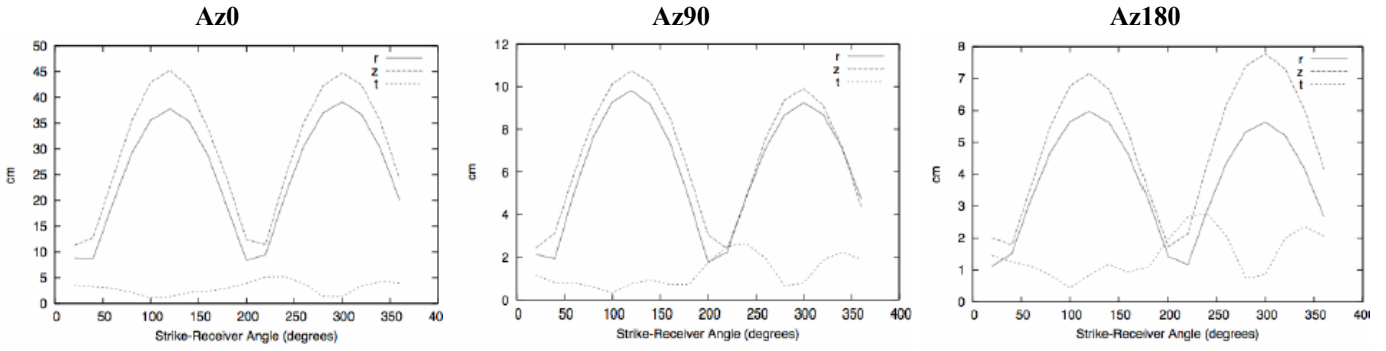


Figure 16: Variation of PGD (cm) with strike for the three components of motion (radial, transverse and vertical) and for a site in forward (Az0), neutral (Az90) and reverse (Az180) directivity condition for a bilateral rupture

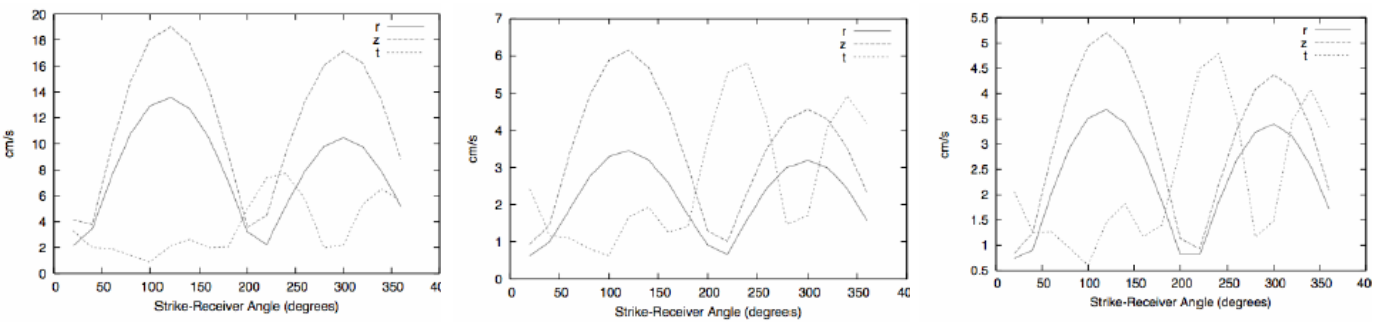


Figure 17: Variation of PGV (cm/s) with strike for the three components of motion (radial, transverse and vertical) and for a site in forward (Az0), neutral (Az90) and reverse (Az180) directivity condition for a bilateral rupture

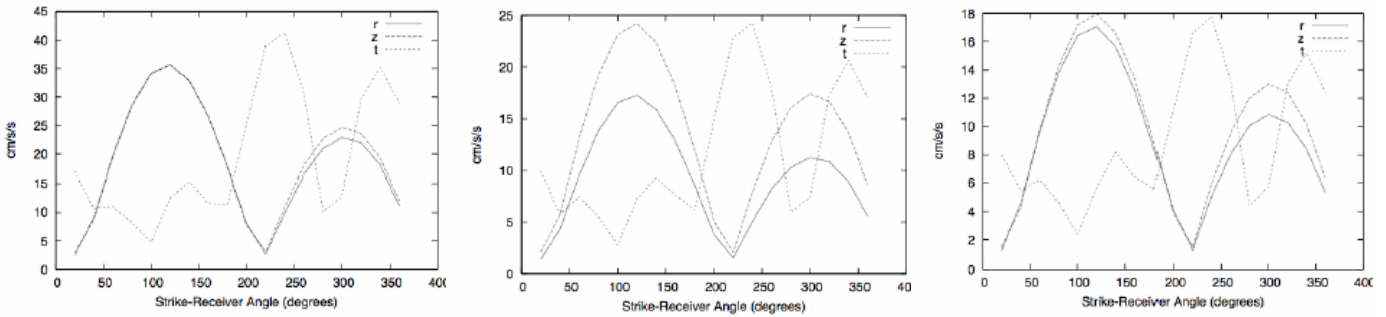


Figure 18: Variation of PGA (cm/s/s) with strike for the three components of motion (radial, transverse and vertical) and for a site in forward (Az0), neutral (Az90) and reverse (Az180) directivity condition for a bilateral rupture

#### 4.4 1985 EVENT AT VALPARAISO

The receiver is supposed to be in the Valparaiso urban area, at an epicentral distance of about 30 km. In the next figures, examples of the results of the parametric studies that have been performed changing the strike-receiver ( $\phi$ ), the dip ( $\delta$ ), the rake ( $\lambda$ ) angles, the hypocentral depth ( $h$ ), and directivity condition, are shown for SSPS and STSPS. The results of these parametric studies allow us to fix some of the focal mechanism parameters that will be used in Section 6 for the computation of synthetic signals along detailed profiles for this scenario earthquake.

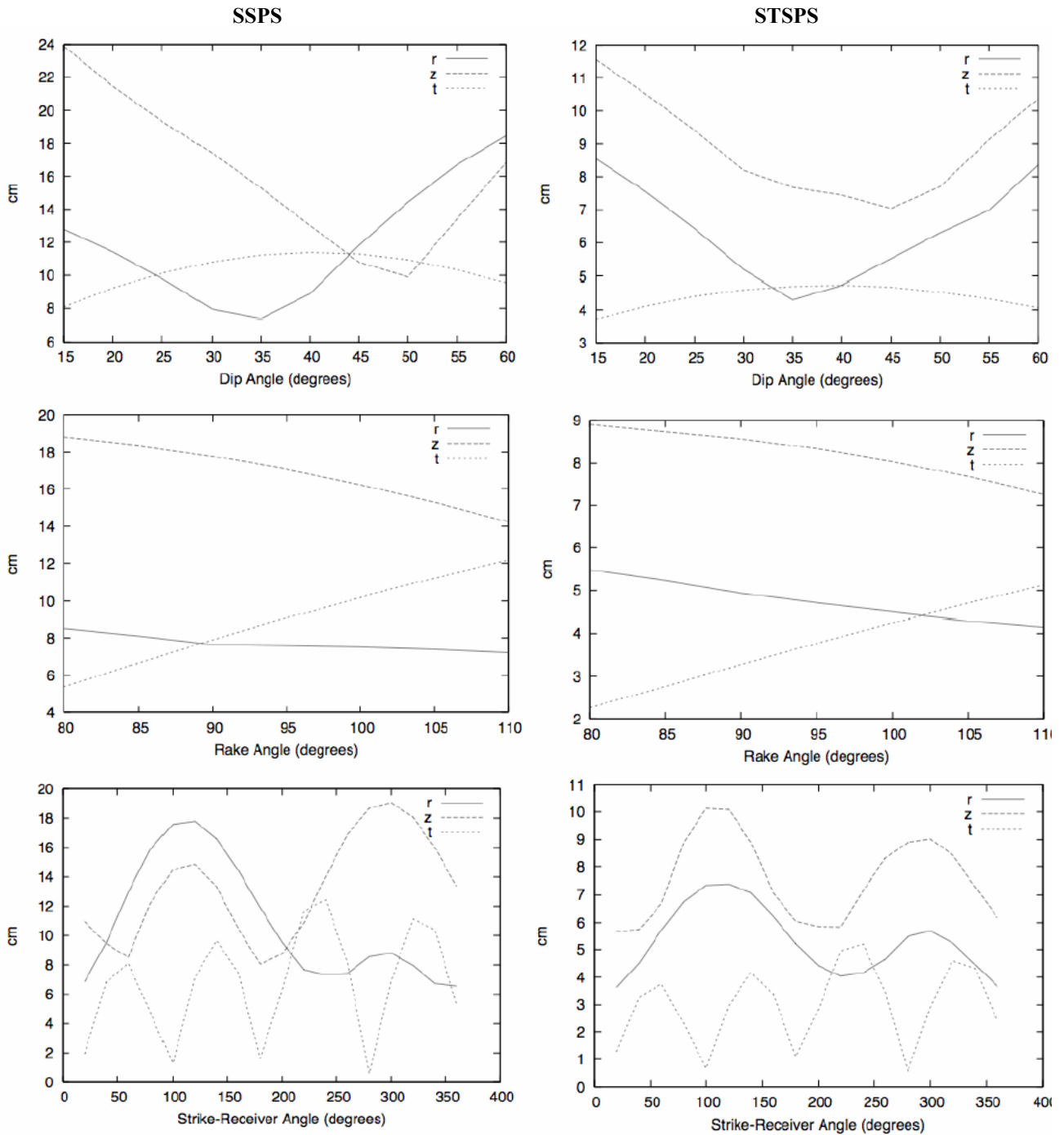


Figure 19: Variation of PGD (cm) with strike, dip and rake for the three components of motion (radial, transverse and vertical); SPSS and STSPS.

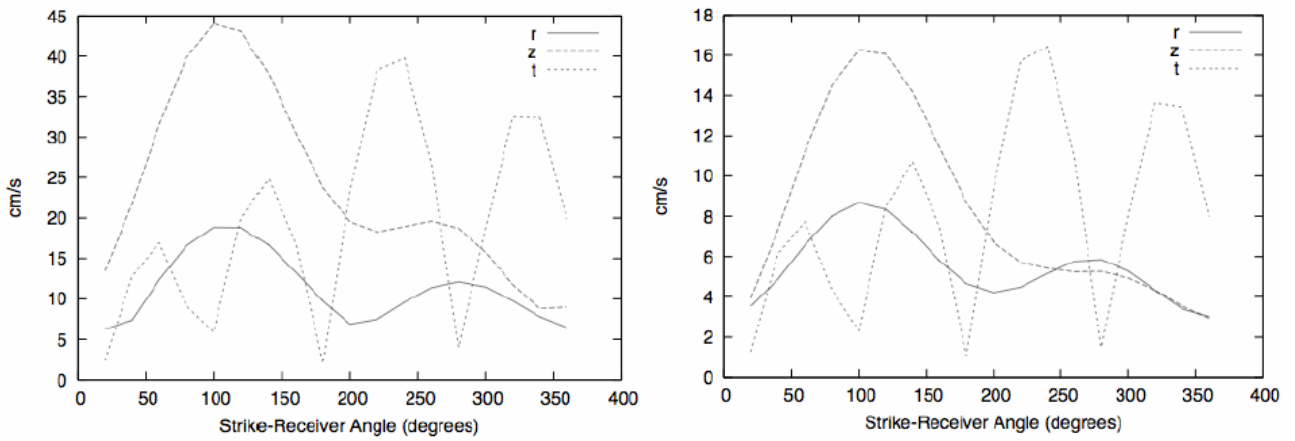


Figure 20: Variation of PGV (cm) with strike for the three components of motion (radial, transverse and vertical); SPSS and STSPS

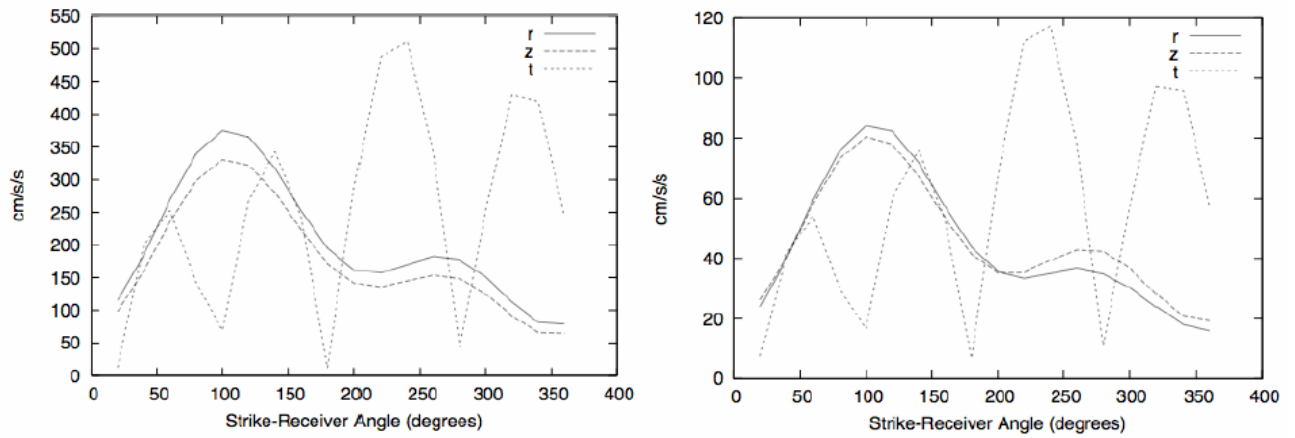


Figure 21: Variation of PGV (cm) with strike for the three components of motion (radial, transverse and vertical); SPSS and STSPS.

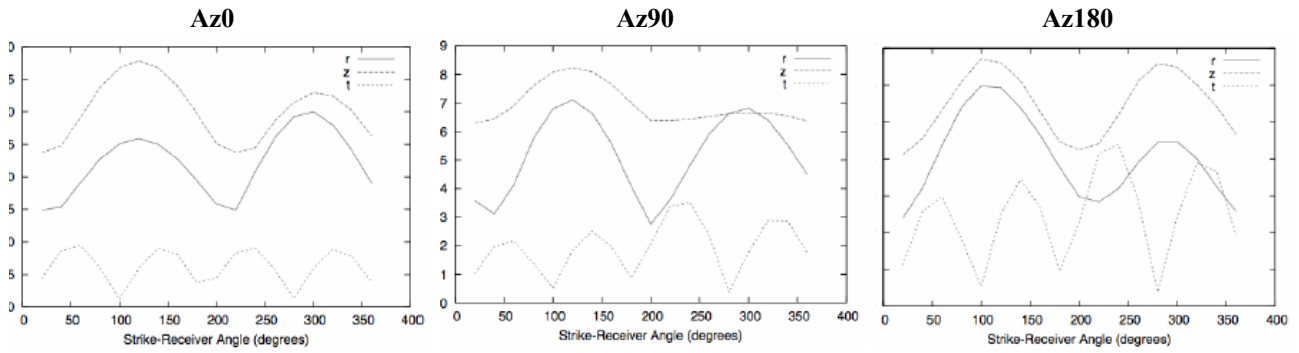


Figure 22: Variation of PGD (cm) with strike for the three components of motion (radial, transverse and vertical) and for a site in forward (Az0), neutral (Az90) and reverse (Az180) directivity condition for a unilateral rupture

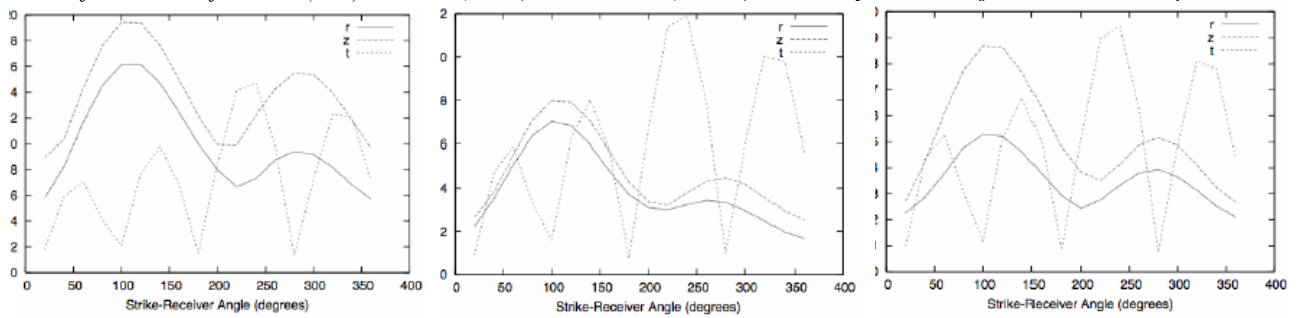


Figure 23: Variation of PGV (cm) with strike for the three components of motion (radial, transverse and vertical) and for a site in forward (Az0), neutral (Az90) and reverse (Az180) directivity condition for a unilateral rupture

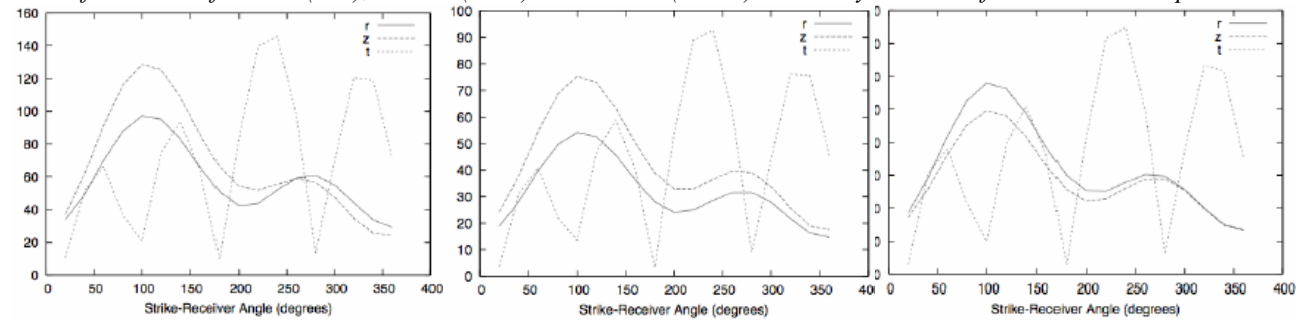


Figure 24: Variation of PGA (cm) with strike for the three components of motion (radial, transverse and vertical) and for a site in forward (Az0), neutral (Az90) and reverse (Az180) directivity condition for a unilateral rupture

## 4.5 VALIDATION

Quantitative validation of the deterministic results has been made using the only available observed signals in Valparaiso urban zone, i.e. the ones recorded during the 1985 earthquake at the El Almendral and Universidad Santa Maria recording stations (e.g. Saragoni, 2006).

Many investigators have studied the source parameters of the Chilean earthquake of March 3, 1985 (e.g. Beresnev and Atkinson, 1997; Somerville et al., 1991) and in Figure 25 an example of extended source model, with the geographical reference, is shown. In this study, we have chosen the one proposed by Choy and Dewey (1988), with a strike of  $360^\circ$ , a dip  $35^\circ$ , a rake of  $105^\circ$  and the result given by the CMT Catalogue of Harvard (<http://www.globalcmt.org/>).

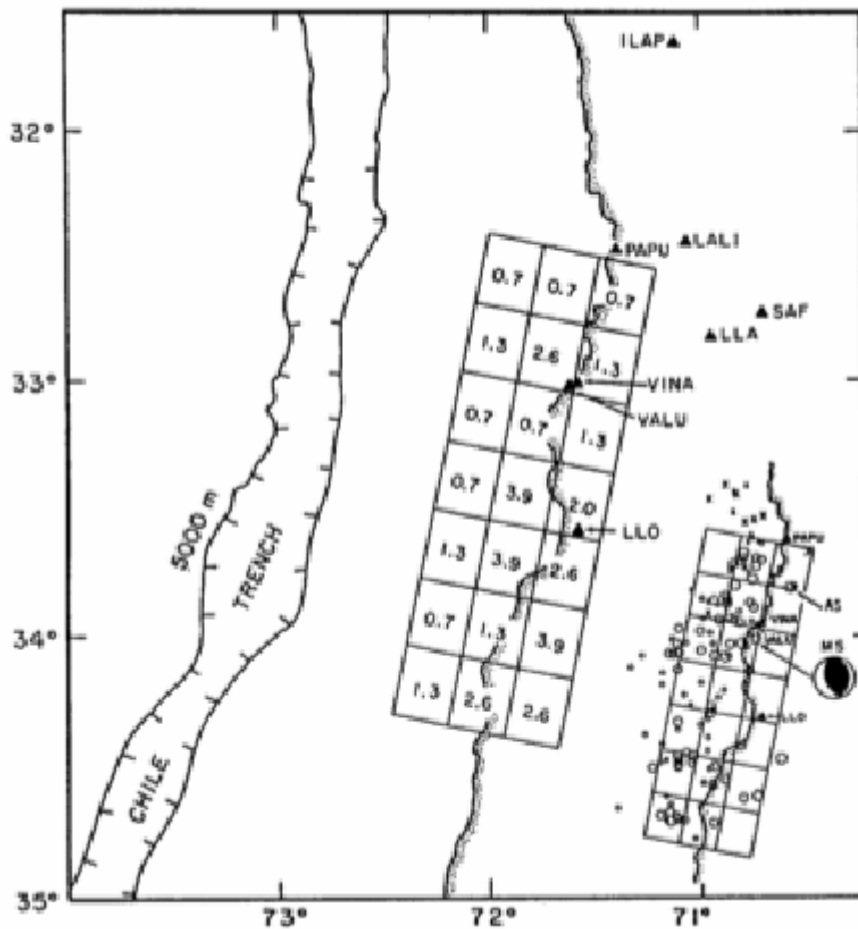
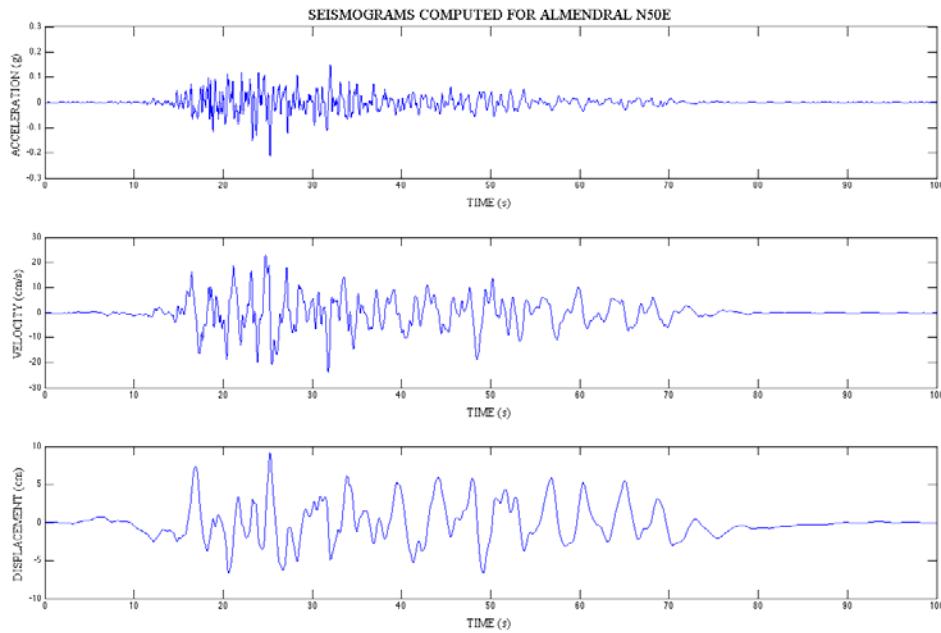


Figure 25: source and station geometry for the 1985 Valparaiso, Chile, earthquake: map view showing horizontal projection of fault; numbers in fault elements represent slip in meters (from Somerville et al., 2001).

Figure 26a shows the first “blind” simulated seismograms (respectively displacement, velocity and acceleration) along the NS and EW components using the extended source models embedded in the bedrock structural model and calculated at the El Almendral station. The signals recorded at such a station, located on a sedimentary cover, are shown in Figure 26b and confirm that the extended source and bedrock models allow to reproduce the observed amplitude and duration of the ground motion. The comparison between the simulated and the recorded signals, and the related response spectra, at the UTFSM station (located on bedrock) are shown in Figure 27, that demonstrates how the agreement is really good. Table 2 summarizes the results of this “blind”, i.e. without any tuning process, validation procedure, confirming that the extended source and bedrock models are successfully validated for the computation of the seismic input (Sections 5 and 6).

Table 2: Peak ground motion values for (blind) simulated and observed signals										
RECEIVERS	COMPONENTS	CHOY			CMT			OBS		
		Amax (g)	Vmax (cm/s)	Dmax (cm)	Amax (g)	Vmax (cm/s)	Dmax (cm)	Amax (g)	Vmax (cm/s)	Dmax (cm)
EL ALMENDRAL	N50°E	0.1516	23.05	9.16	0.128	12.07	6.22	0.2907	28.59	5.37
	S40°E	0.1640	14.07	6.10	0.122	15.23	5.32	0.1621	16.89	2.81
U.T.F.S.M	N70°E	0.1467	20.49	7.55	0.112	11.38	5.79	0.1767	14.70	3.26
	S20°E	0.1399	14.07	4.54	0.139	18.94	5.68	0.1625	6.40	1.33

a)



b)

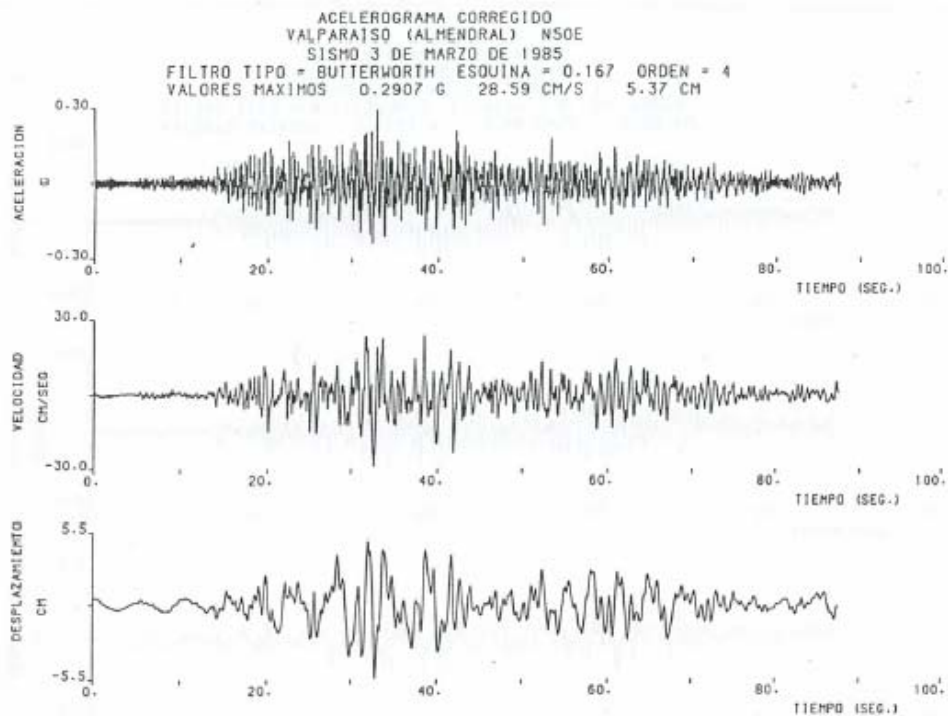
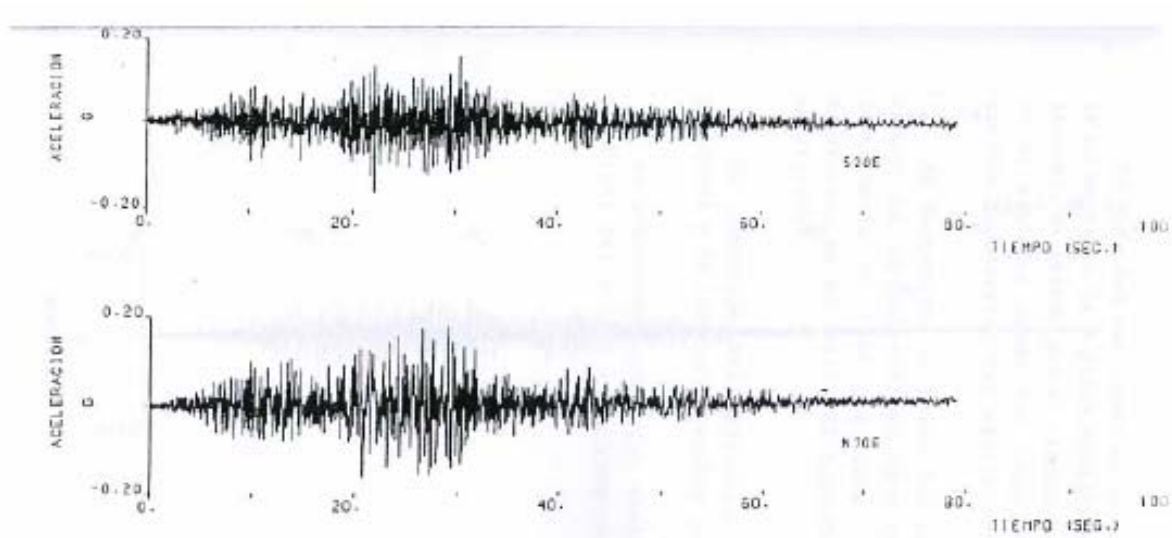
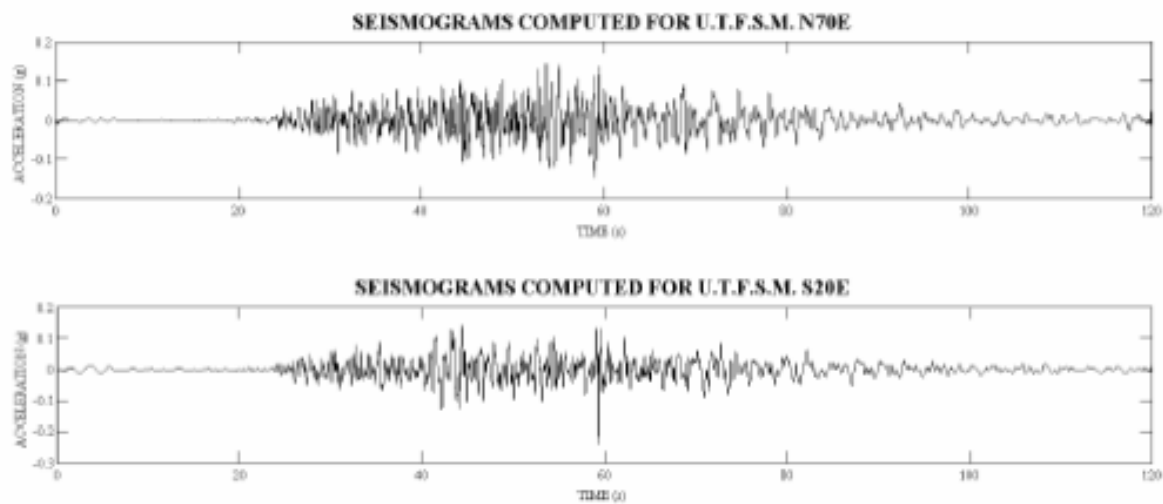


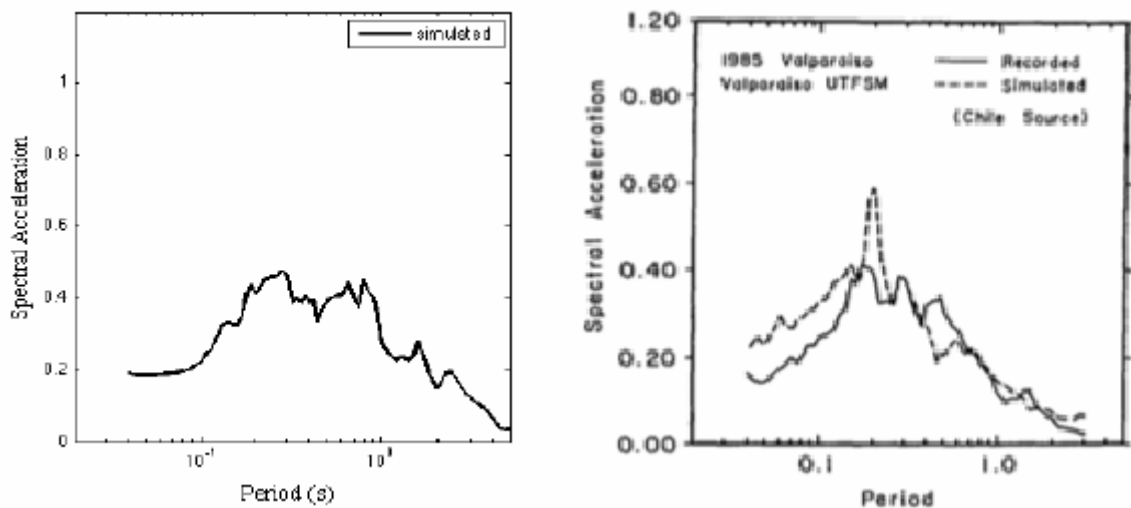
Figure 26: El Almendral station: acceleration, velocity and displacement for the 1985 event. a) computed (unilateral rupture; b) recorded.



a)



b)



c)

Figure 27: 1985 event at UTFSM station: a) Horizontal recorded accelerations; b) simulated accelerations; c) comparison of response spectra: this study, recorded and the one simulated by Somerville et al., 1991.



## 5. SEISMIC INPUT AT URBAN SCALE

The methodology, explained in Section 3, for the extended source representation and the source models, discussed and validated in Section 4, allow us to generate a set of groundshaking scenarios in the urban area of Valparaiso, associated to different “scenario” earthquakes. The scenario earthquakes that can be classified, according to their different: a) magnitude, b) occurrence period,  $T_m$ , to be intended solely for an engineering analysis, and c) risk level:

Magnitude 7.5	Occasional ( $T_m \approx 120-140$ years, Strong)
Magnitude 7.8 (1985)	Sporadic ( $T_m \approx 200-250$ years, Very Strong)
Magnitude 8.3 (1906)	Rare ( $T_m \approx 500$ years, Disastrous)
Magnitude 8.5	Exceptional ( $T_m \approx 1000$ years, Catastrophic)

For every scenario two rupture styles (unilateral North to South and bilateral) have been considered and the synthetic signals (displacements, velocities and accelerations) for the two horizontal components of motion (N-S and E-W) have been computed at a dense grid (step of approximately 0.02 km) of sites in the Valparaiso urban area. The peaks of the ground motion, and their period of occurrence, have been extracted in a matrix form; these results have been delivered (see annexed “GIS data”) to UR ENEA to be GIS processed and graphically rendered in a set of 96 maps (see UR ENEA report). As an example, Figures 28-29 show some of the results, that are extremely important since the information they carry can be mapped in terms of Intensity scenarios and thus they can be compared with the available measured intensities for the 1985 and 1906 scenarios. Panza et al. (1997) have produced new relations between Intensity,  $I$ , and the peak values of acceleration, velocity and displacement, valid for the Italian territory. They used two different versions of the GNDT earthquake catalogue (NT3.1 and NT4.1.1) and two sets of observed intensity maps for the Italian territory (ING and ISG data) and exploited advanced modeling methods for seismic waves propagation (Panza et al., 2001). The results obtained for accelerations do not differ significantly from the earlier results of Cancani (1904). From Table 3 and 4, it is evident that the generated groundshaking scenarios match very well the average intensities measured in Valparaiso for the 1985 (VIII MSK) and the 1906 (IX MSK) as reported by Saragoni (2006) and Astroza (2006).

Intensity	Displacement (cm)	Velocity (cm/s)	DGA (g)
V	0.1 – 0.5	0.5 – 1.0	0.005 – 0.01
VI	0.5 - 1.0	1.0 – 2.0	0.01 – 0.02
VII	1.0 – 2.0	2.0 – 4.0	0.02 – 0.04
VIII	2.0 – 3.5	4.0 – 8.0	0.04 – 0.08
IX	3.5 – 7.0	8.0 – 15.0	0.08 – 0.15
X	7.0 – 15.0	15.0 – 30.0	0.15 – 0.30
XI	15.0 – 30.0	30.0 – 60.0	0.30 – 0.60

Intensity	Displacement (cm)	Velocity (cm/s)	DGA (g)
VI	1.0 – 1.5	1.0 – 2.0	0.01 – 0.025
VII	1.5 – 3.0	2.0 – 5.0	0.025 – 0.05
VIII	3.0 – 6.0	5.0 – 11.0	0.05 – 0.1
IX	6.0 - 13.0	11.0 – 25.0	0.1 – 0.2
X	13.0 – 26.0	25.0 – 56.0	0.2 – 0.4

*Table 5. Adapted from Dolce et al., 2005. Comparison of seismic intensity scales;  
MM – Modified Mercalli; RF – Rossi-Forel; JMA – Japanese Meteorological Agency;  
MCS – Mercalli-Cancani-Sieberg; MSK – Medvedev-Sponheuer-Karnik*

MM	RF	JMA	MCS	MSK
I	I	I	II	I
II	II		III	II
III	III		IV	III
IV	IV	II	V	IV
V	V	III	VI	V
	VI		VII	VI
VI	VII	IV	VIII	VII
VII	VIII	V	IX	VIII
VIII	IX		X	IX
IX		X	VI	XI
X	X		VII	XII
XI		XII		XII
XII				

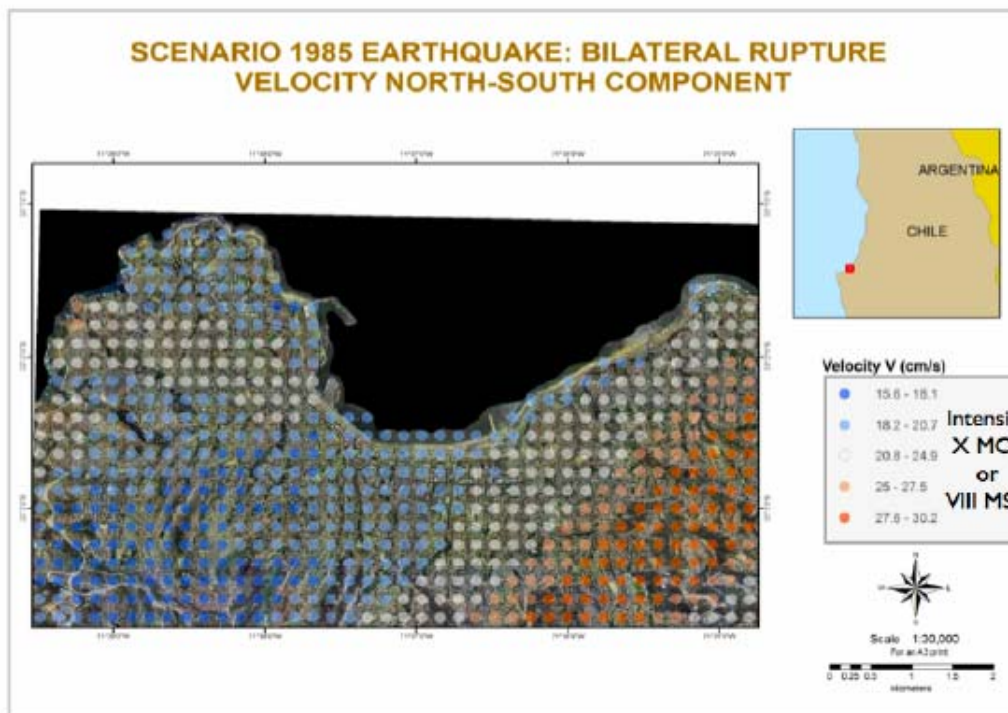


*Figure 28: Groundshaking scenario in the Valparaiso urban area for the 1985 event.  
NS component of velocities for bilateral rupture.*

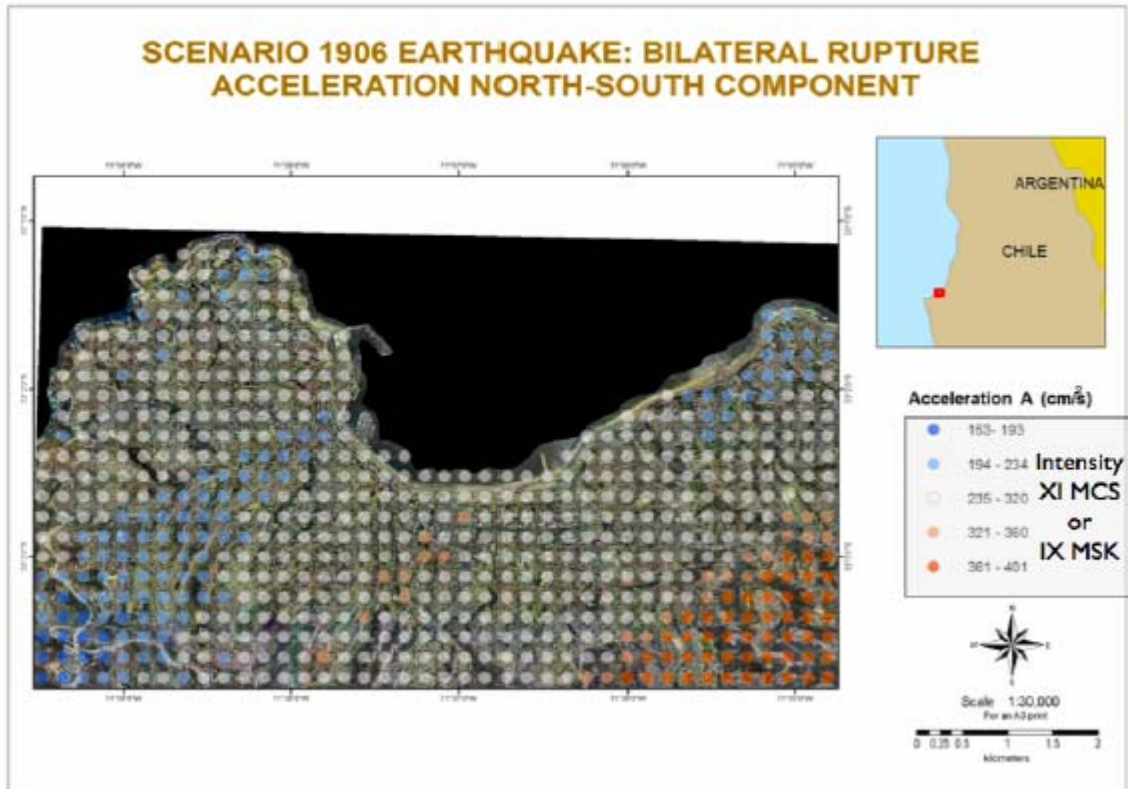


Figure 29: Groundshaking scenario in the Valparaíso urban area for the 1985 event. NS component of accelerations for bilateral rupture.

At the coordinates (collected in November 2007 during to the GPS campaign) of three sites, selected as strategic targets for the whole project, i.e. the three churches La Matriz, San Francisco and Las Hermanitas de la Providencia (see Figure 30), the full seismic input at the bedrock has been specifically computed (see annexed “Engineer data”). The acceleration time histories (and the related response spectra) of the three components of motion computed for the four scenario earthquakes (and two possible ruptures each) have been delivered to UR UNIPD and UR UNIFE for the dynamic engineering analysis.



Figure 30: location of the 3 Churches, selected as target sites in the Valparaíso urban area

As an example, in Figure 31 the time histories computed for the 1906 scenario (unilateral rupture) at the La Matriz church are shown; it is the only one located (see Figure 33 in Section 6) on a bedrock site, while the other two churches are located near the El Almendral area characterized by the presence of a sedimentary basin. The computation of the seismic input at sites that can be affected by local soil amplifications is discussed in Section 6.

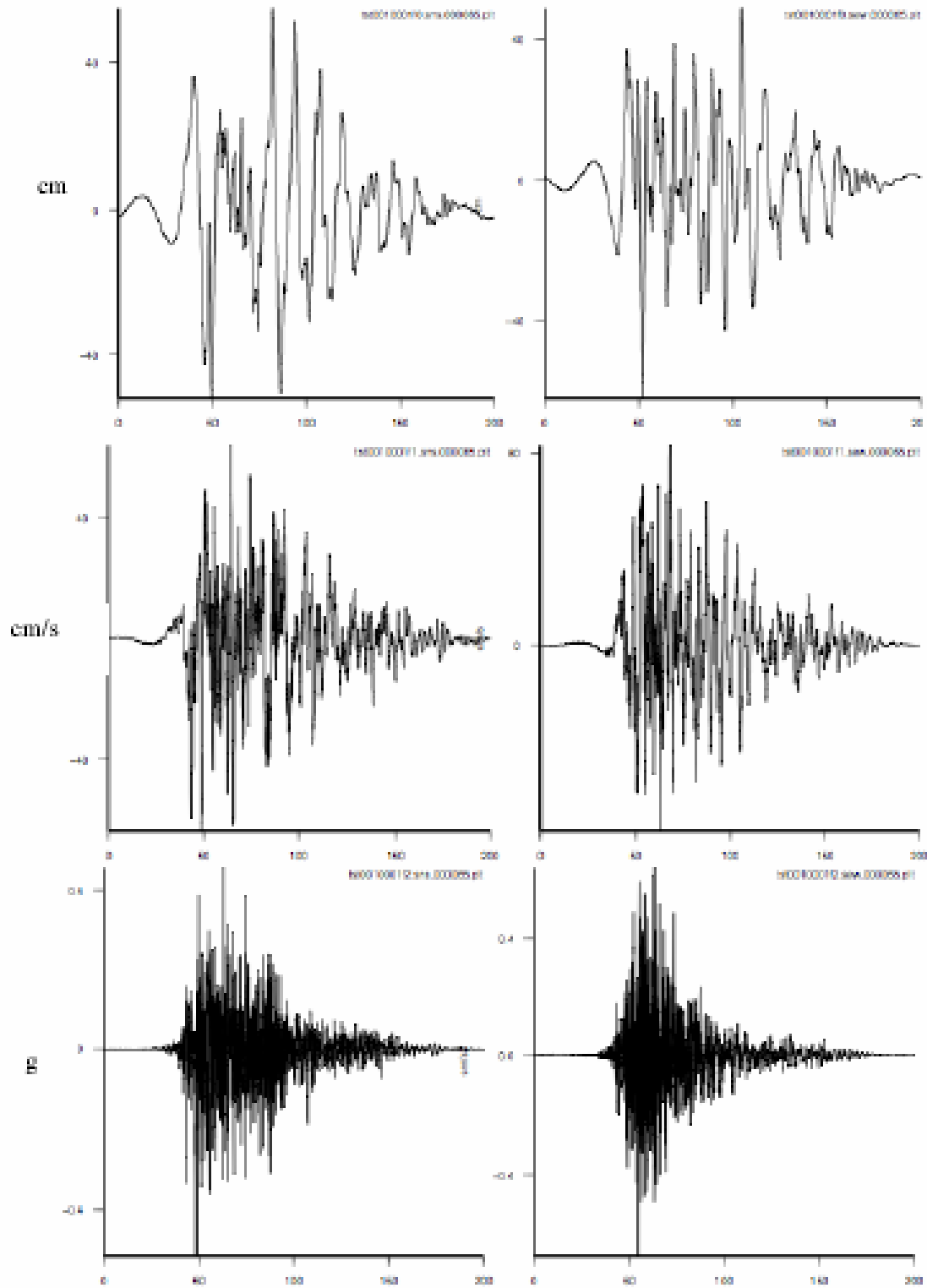


Figure 31: Example of seismic input computed at the La Matriz church: 1906 scenario, bilateral rupture. Displacements, velocities and accelerations for the two horizontal components of motion.

## 6. SEISMIC INPUT ALONG SELECTED PROFILES: SITE RESPONSE ESTIMATION

To deal both with realistic source and structural models, including topographical features, a hybrid method has been developed that combines modal summation and the finite difference technique (e.g. Fäh et al., 1993, 1994), and optimizes the use of the advantages of both methods. Wave propagation is treated by means of the modal summation technique from the source to the vicinity of the local, heterogeneous structure that we may want to model in detail. A laterally homogeneous anelastic structural model is adopted, that represents the average crustal properties of the region. The generated wavefield is then introduced in the grid that defines the heterogeneous area and it is propagated according with the finite differences scheme. With this approach, source, path and site effects are all taken into account, and it is therefore possible a detailed study of the wavefield that propagates even at large distances from the epicentre. This methodology has been successfully applied to many urban areas spread worldwide (e.g. Panza et al., 1999; Zuccolo, 2008), to strategic buildings and lifelines (e.g. Romanelli et al., 2003; 2004; Vaccari et al., 2005).

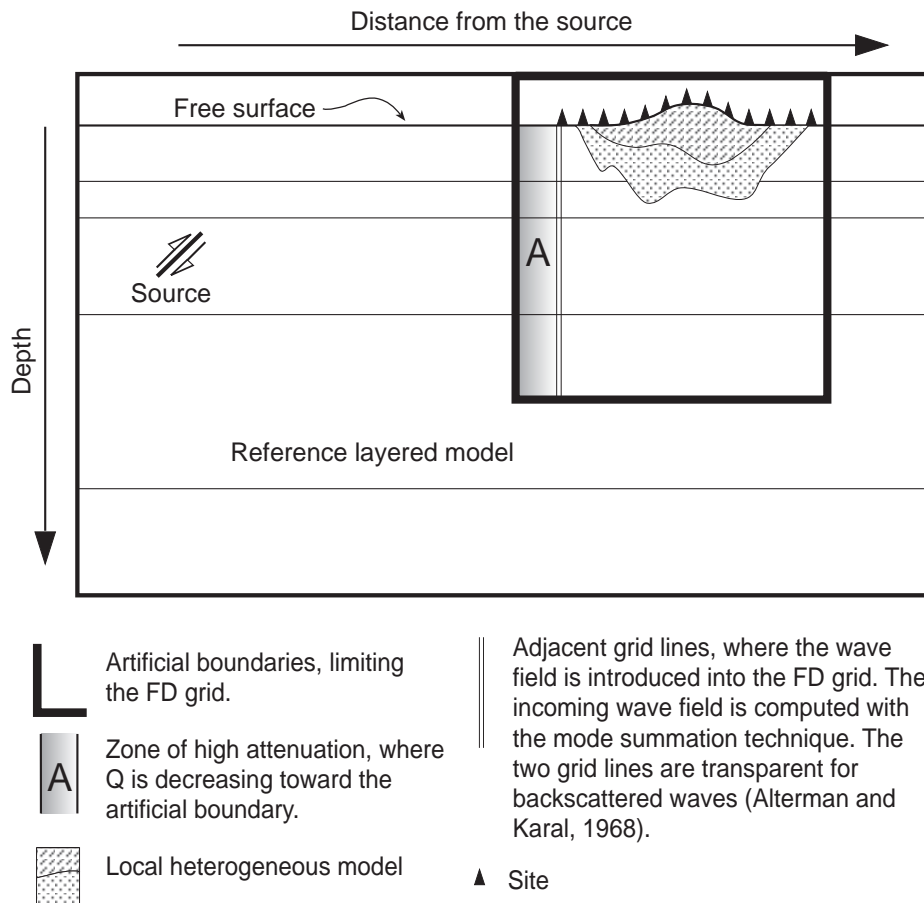


Figure 32: scheme of the hybrid (modal summation plus finite differences) method.

In the hybrid scheme, two local heterogeneous models have been coupled with the average regional model used in the initial (see Section 2) analysis for the detailed modelling of earthquake ground motion by computing synthetic seismograms in laterally heterogeneous media. The two profiles, about 2 km long and 0.2-0.4 km deep each, have been selected according to the available information and to their representativeness of the most important areas of the municipality (see Figure 33). To define the sub-surface topography of the sedimentary layers we have used and elaborated the bedrock model of Verdugo (1995), the information given by Espinoza (2000).

We have then performed some parametric tests, i.e. a) including or not some very superficial layers, b) changing the values of elastic and anelastic parameters, c) choosing different bedrock models and d) adopting the different scenarios defined in Section 5. In the following we show the results related to the two profile models shown in Figure 34, together with the values of the adopted elastic and anelastic parameters. The minimum S-wave velocity present in the models shown is 660 m/s, and the mesh used for the finite differences is defined with a grid spacing of 7 m. This allows us to carry out the computations at frequencies as high as about 10 Hz. The synthetic time signals (displacements, velocities and accelerations) have been calculated for the three components of motion, adopting a STSPS seismic source model for the 1985 earthquake scenario. Site effects are then evaluated as spectral amplifications, described by the ratios (2D/1D) of the acceleration response spectra, with 5% damping, computed along the bedrock model (1D) profile and along the one containing the local model (2D).



Figure 33: Bedrock model (depth) at El Almendral (Verdugo, 1995; Saragoni 2006) and the position of the two profiles.

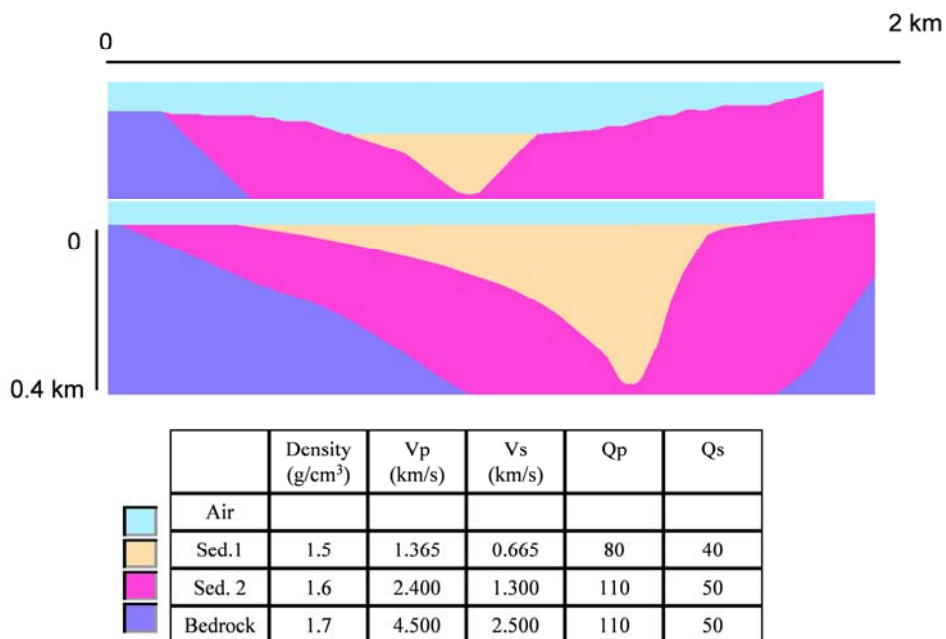


Figure 34: Local profiles (top – red line of Figure 33, bottom – blue line of Figure 33) with their elastic and anelastic parameters.

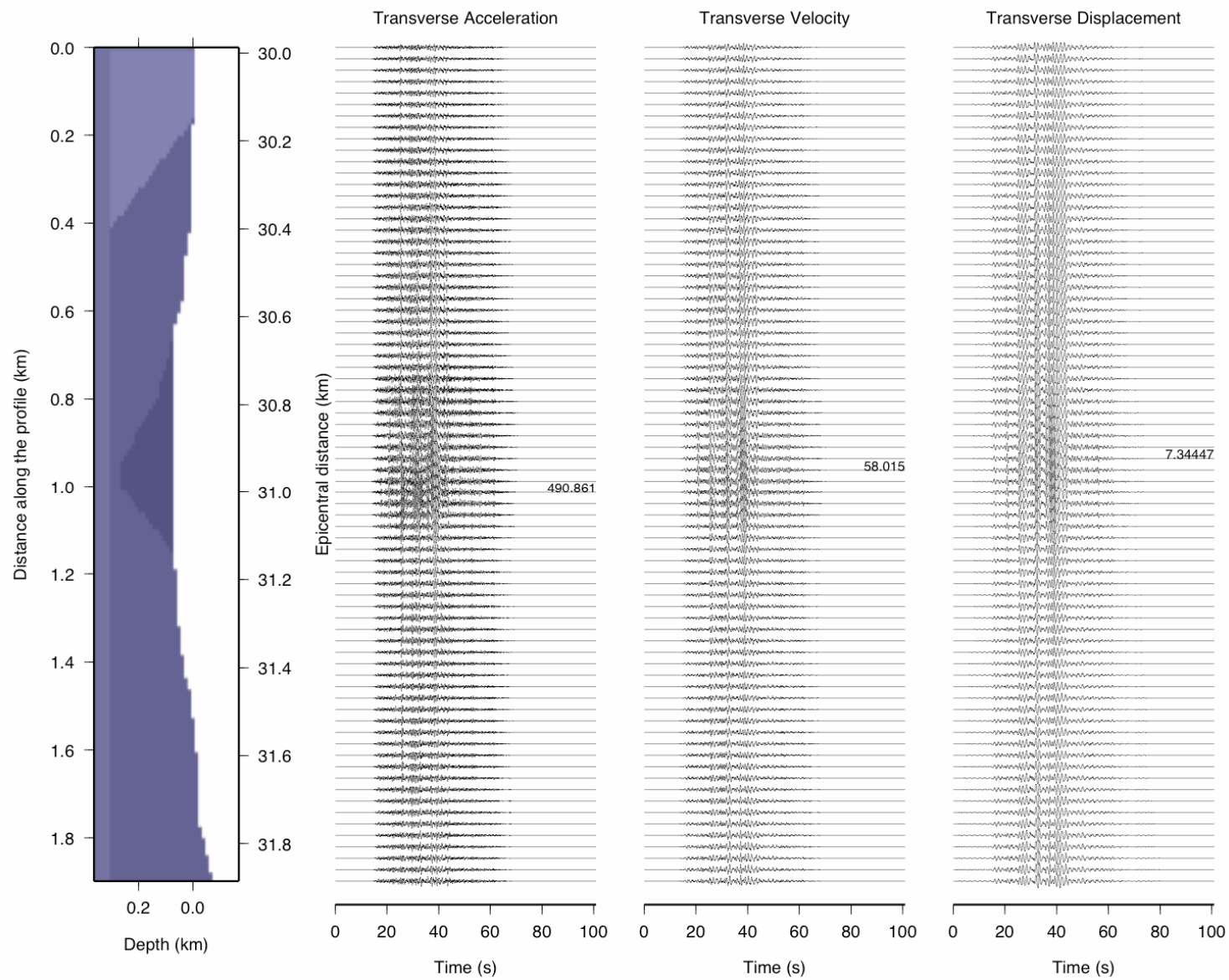


Figure 35: Transverse component of motion along profile 1. 1985 scenario STSPS source model.

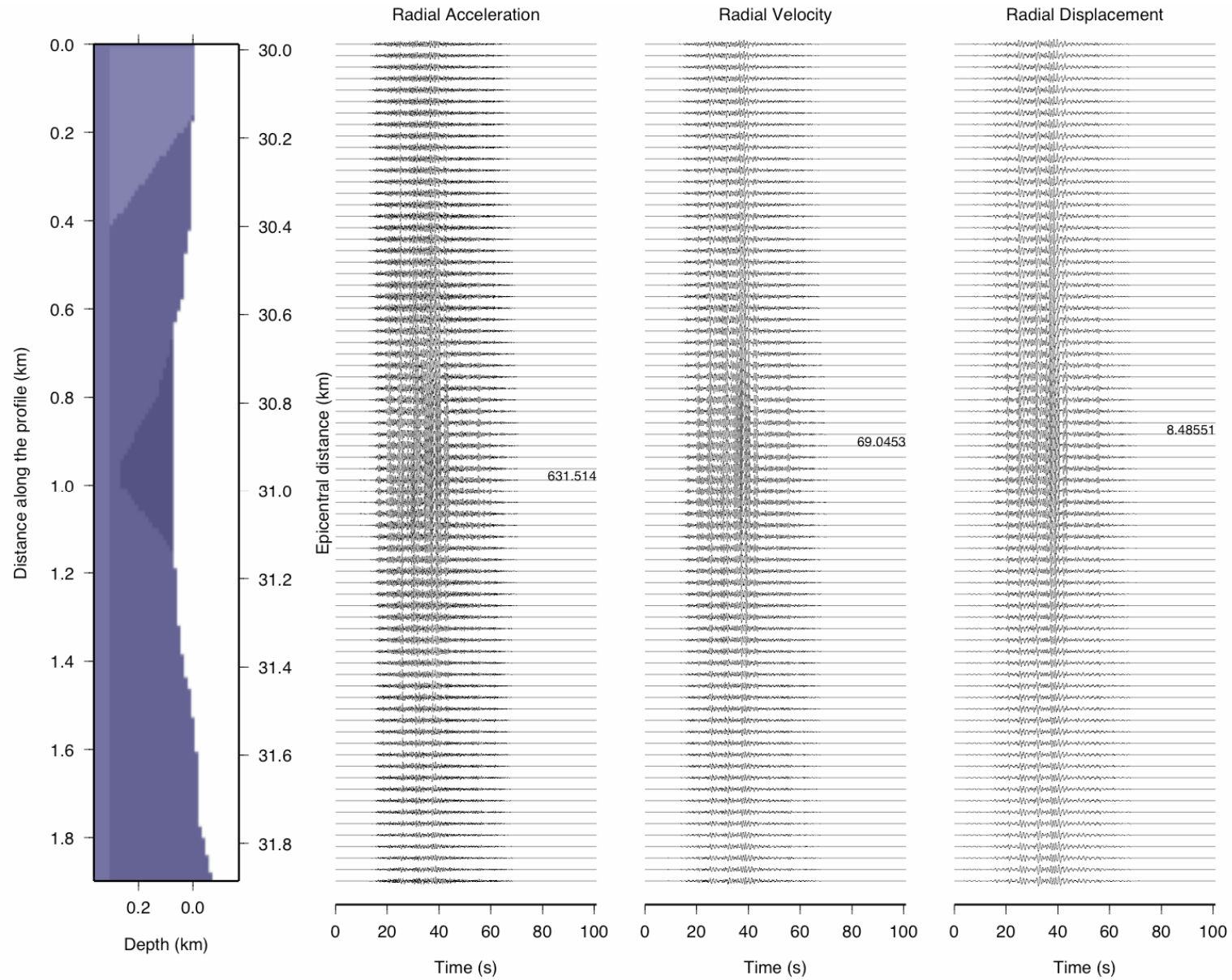


Figure 36: Radial component of motion along profile 1. 1985 scenario STSPS source model.



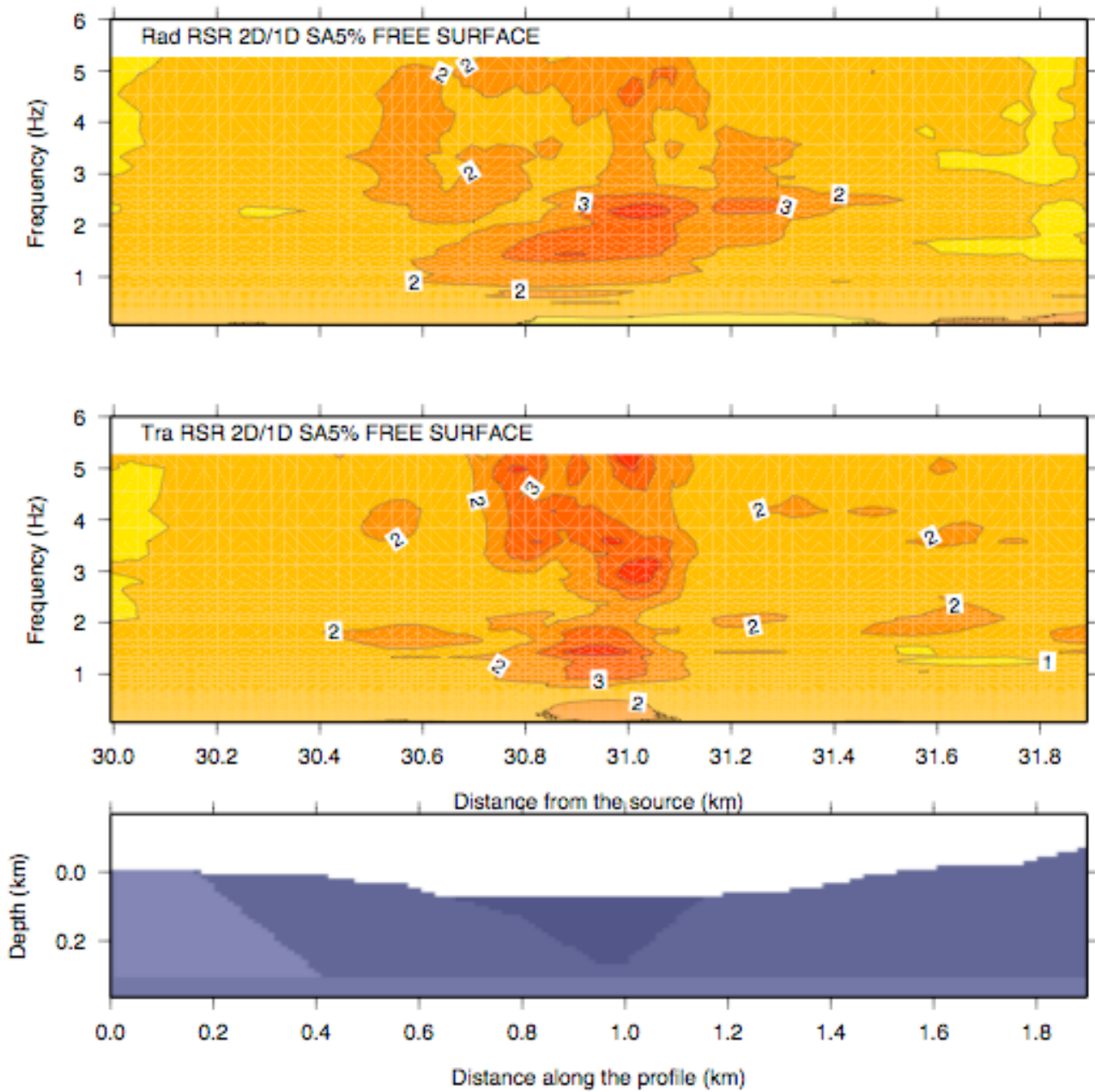


Figure 37: Spectral amplifications obtained along profile 1 for the 1985 scenario. From top to bottom: vertical component, radial component, transverse component.

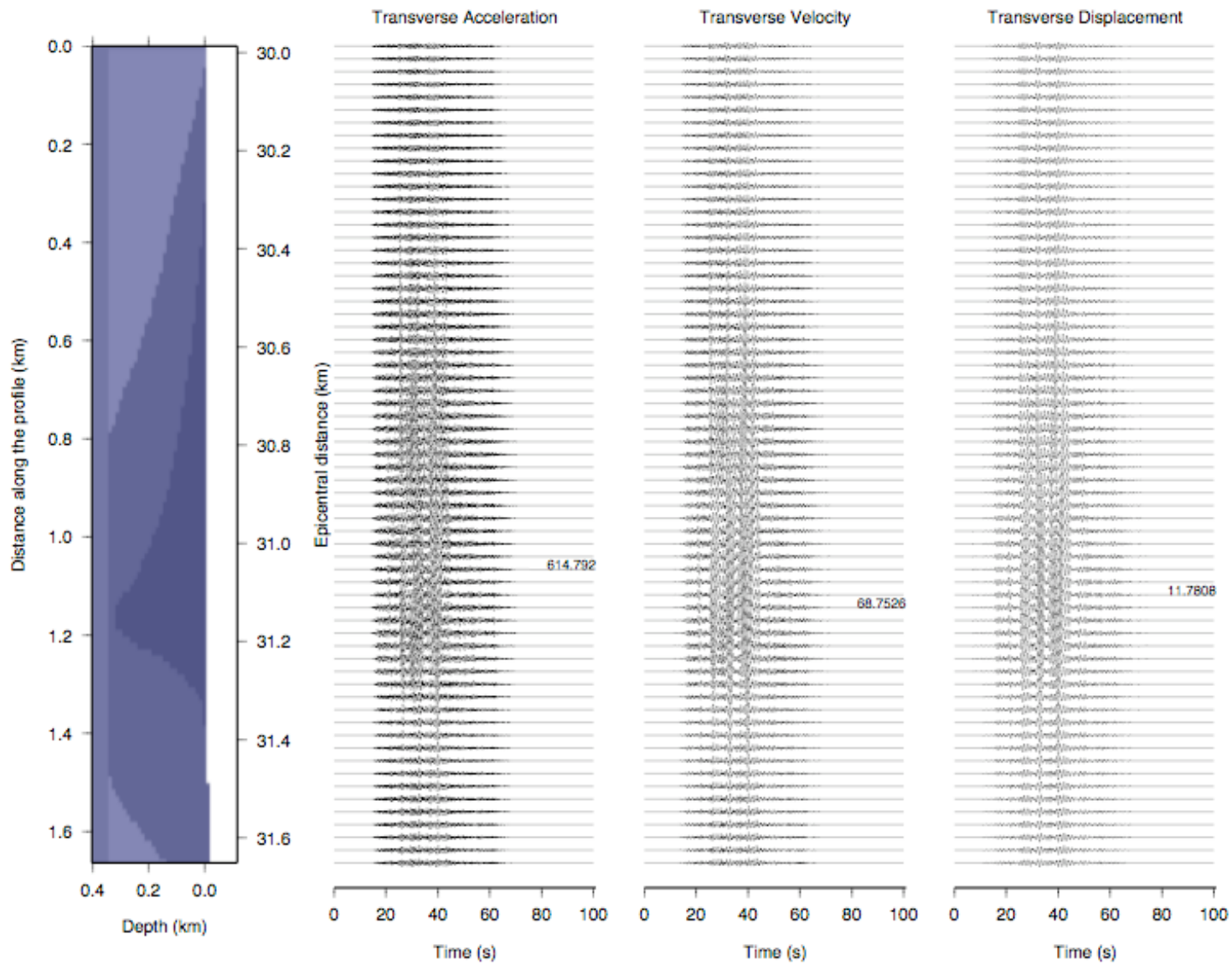


Figure 38: Transverse component of motion along profile 2. 1906 scenario STSPS source model.

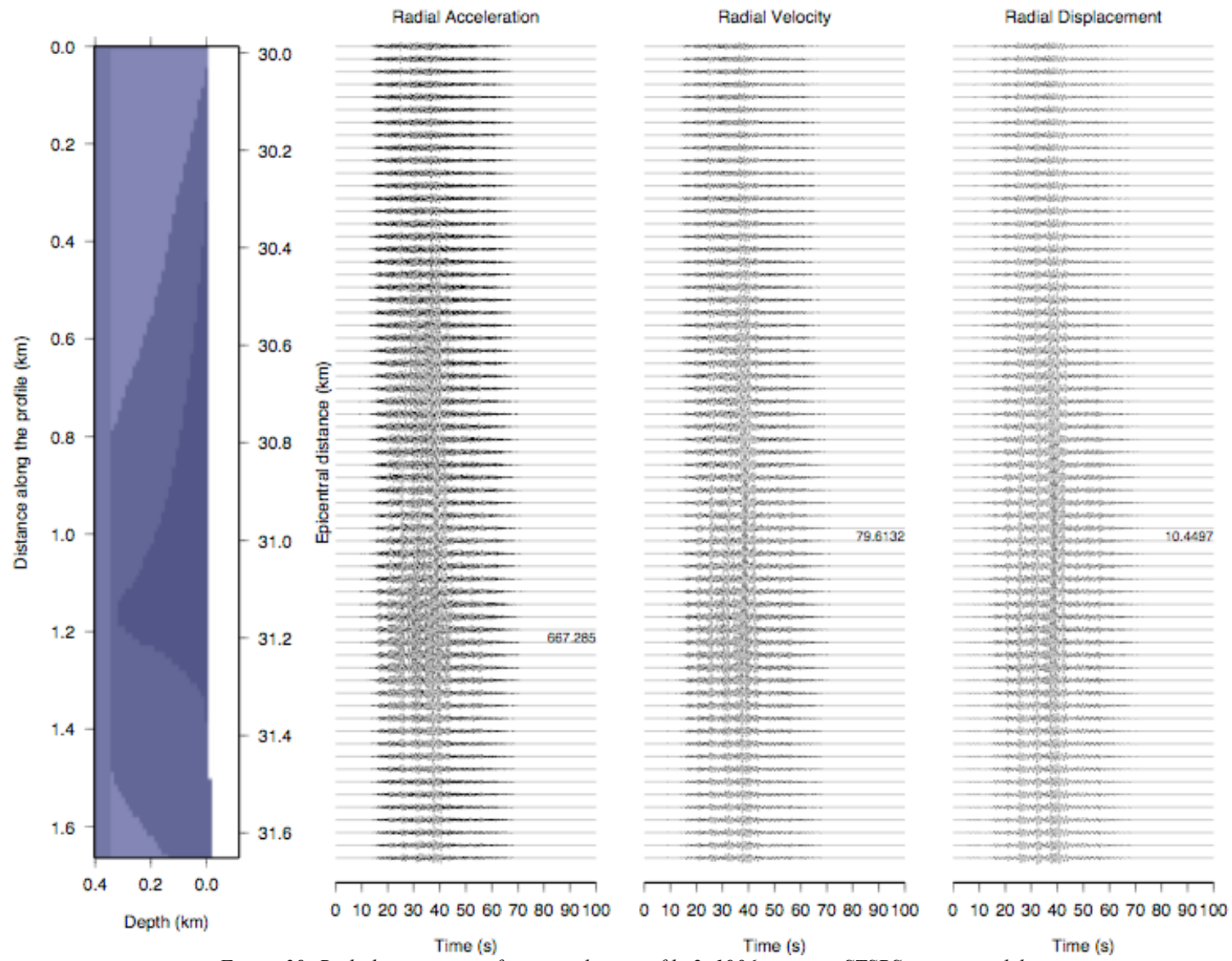


Figure 39: Radial component of motion along profile 2. 1906 scenario STSPS source model.

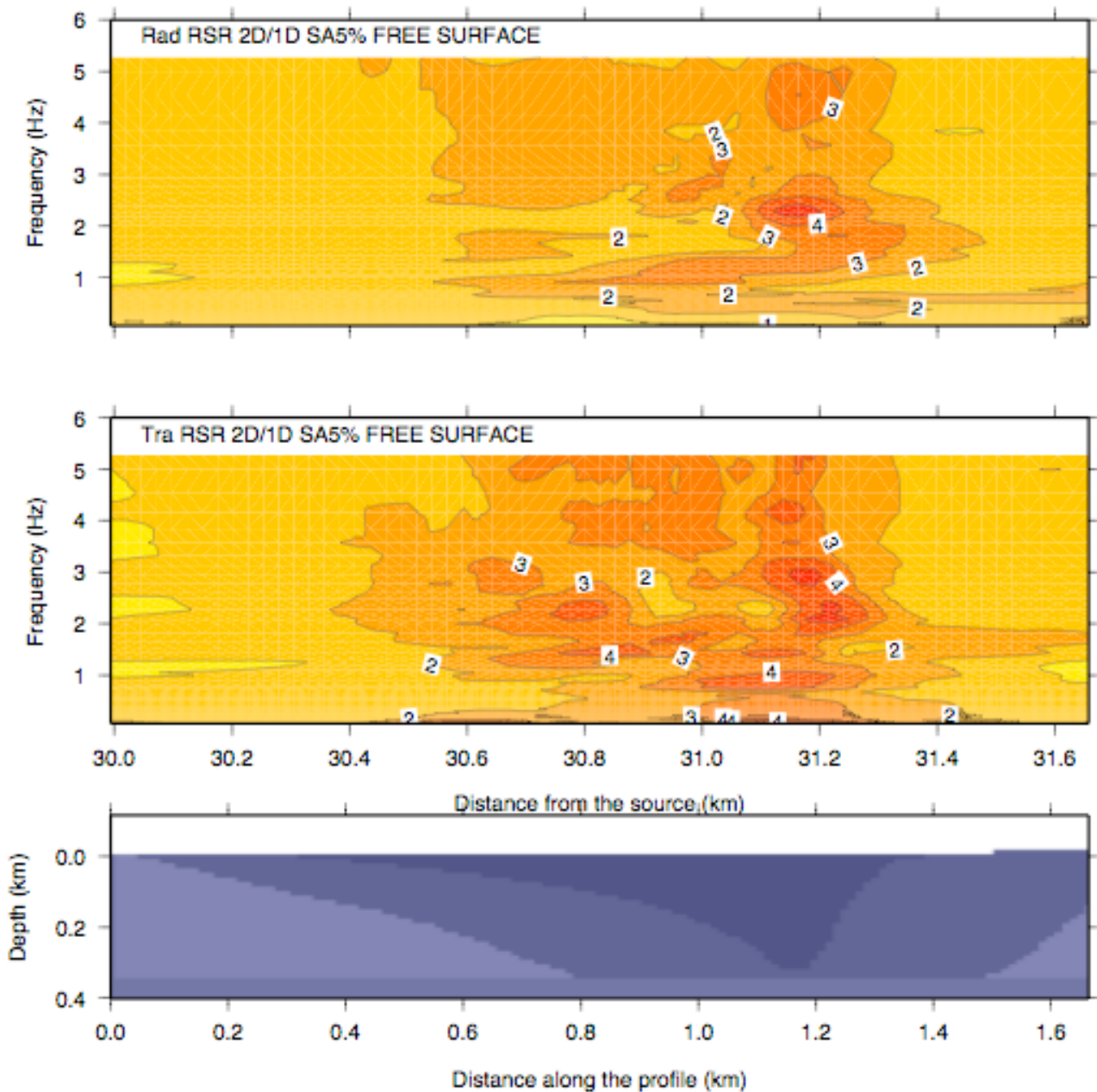


Figure 40: Spectral amplifications obtained along profile 2 for the 1985 scenario. From top to bottom: radial component, transverse component.

The amplification factors computed for the horizontal components (up to 4) explain very well the pattern of the measured intensities in the Valparaíso urban area associated to the 1985 and the 1906 events, as reported for example by Saragoni (2006) and Astroza (2006). In fact, a general result of our investigation is that the local effects due to the thickening of the sedimentary basin (up to 300 m) in the El Almendral zone, can cause an increment greater than 1 unit in the seismic intensity experienced with respect to the average intensity affecting the whole urban area, as clearly shown in Figures 41 and 42.

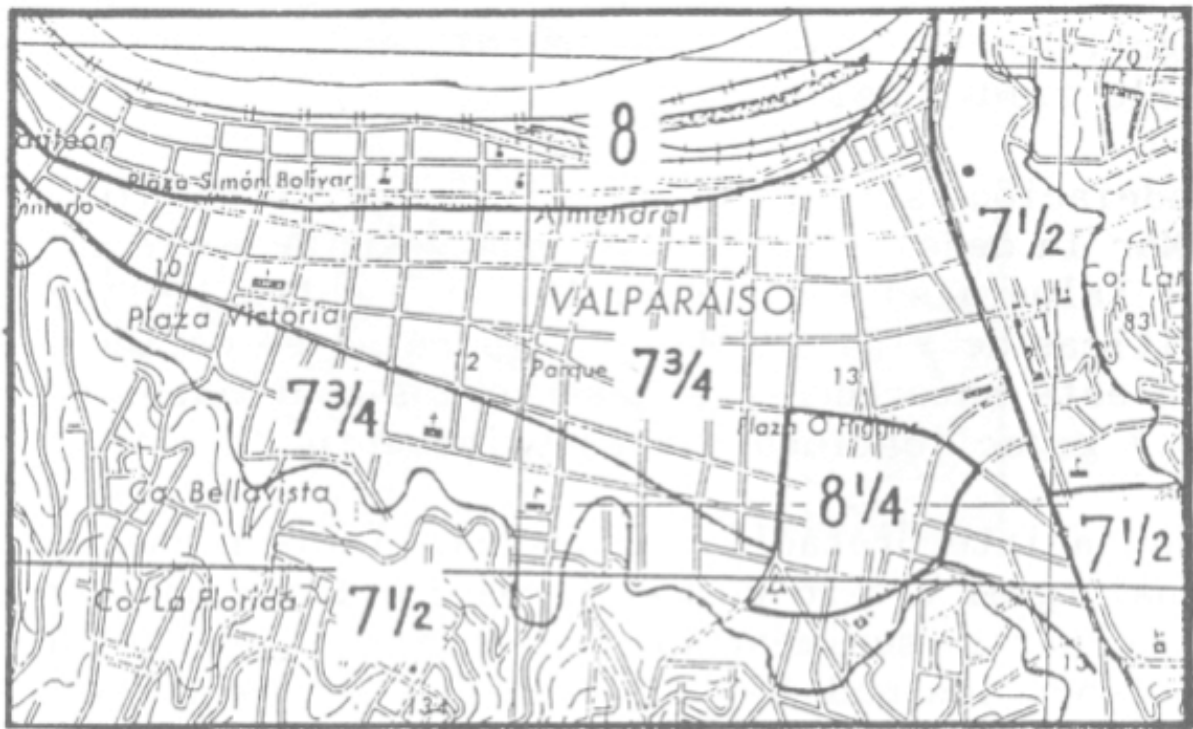


Figure 41: MSK intensities of 1985 Chile Central earthquake at El Almendral (Acevedo et al. 1989).

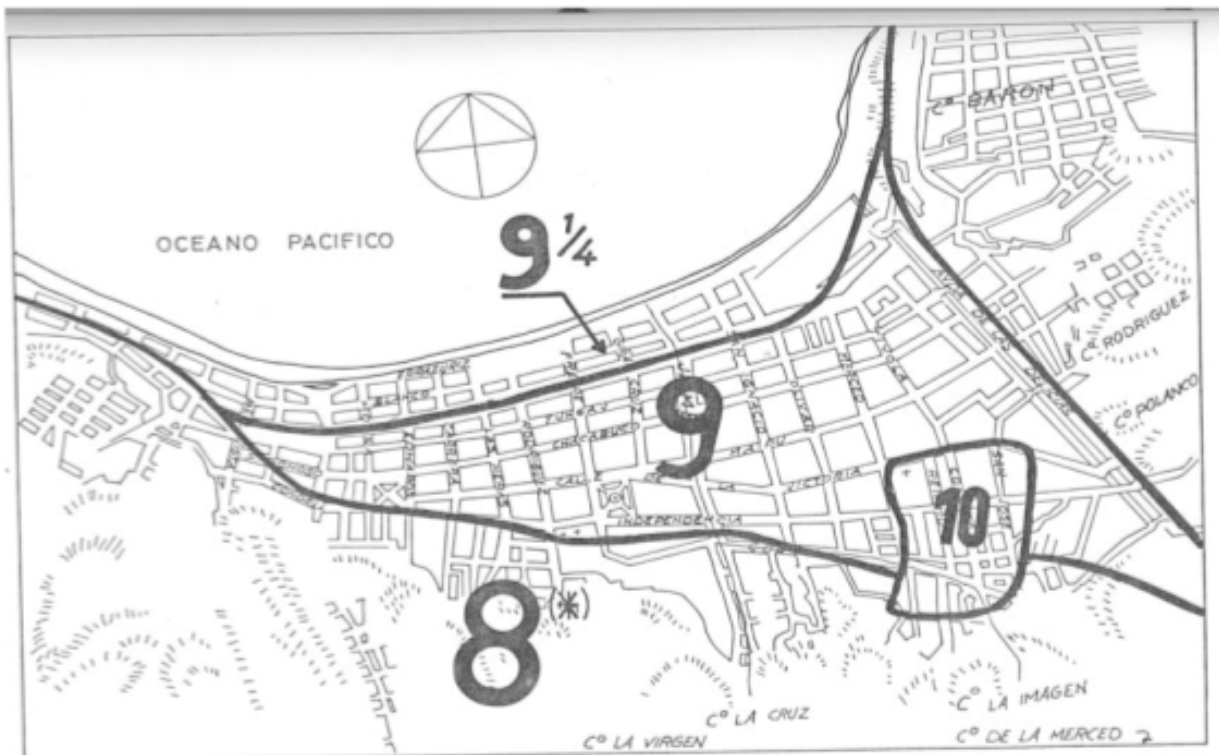


Figure 42: MSK intensities of 1906 earthquake at El Almendral (Saragoni, 2006).

## 7. FINAL REMARKS

The definition of the seismic input in the Valparaiso urban area site, i.e. the determination of the seismic ground motion due to an earthquake with a given magnitude and epicentral distance from the site, has been done following a theoretical approach, that produces results well consistent with the available relevant accelerograms (see Fig. 26 and 27). Such an approach is based on modeling techniques, developed from the knowledge of the seismic source process and of the propagation of seismic waves, that can realistically simulate the ground motion associated with the given earthquake scenario. The synthetic signals, to be used as seismic input in a subsequent engineering analysis, have been produced at a very low cost/benefit ratio taking into account a broad range of source characteristics, path and local (geological and geotechnical) conditions.

The realistic modeling of ground motion requires the simultaneous knowledge of the geotechnical, lithological, geophysical parameters and topography of the medium, on one side, and tectonic, historical, paleoseismological, seismotectonic models, on the other, for the best possible definition of the probable seismic source. The initial stage of the work was thus devoted to the collection of all available data concerning the deep and shallow geology, the construction of cross-sections along which to model the ground motion, and the specification of the possible seismic sources. The analysis of the computed seismic input has been carried out in the time domain (broad band ground motion time series) and in the frequency domain (Fourier and response spectra). We give an estimate of the local response at each site, evaluating the Spectral Ratios, using both the Fourier Spectra (FSR) and Response Spectra (RSR) ratios, for the laterally varying model normalized to the bedrock model. For all of the cases examined, the results show that the lateral heterogeneities can produce strong spatial variations in the ground motion even at small length scales, that can be hardly accounted for by stochastic models commonly adopted in the engineering analysis. Thus, a general result of our modeling is that the effect of the local site conditions can cause an increment greater than 1 unit in the seismic intensity experienced with respect to the average intensity affecting the urban area.

Many parametric studies of the ground motion have been performed, taking into account the variations due to the choice of the focal mechanism parameters, the geometry of the seismic source and the rupture process. Different ground motions at the sites have been studied: a) in order to consider the maximum excitation in both longitudinal and transverse direction, and in order to consider (starting from the Maximum Historical Earthquake) both the Maximum Credible Earthquake and the Maximum Design Earthquake.

### **Acknowledgements**

We used GMT software (Wessel and Smith, 1991) in the preparation of some figures.

## 8. SELECTED REFERENCES FOCUSING ON THE HAZARD IN VALPARAISO

**Most of them have been selected and collected during the *in situ* investigation of the Italian expert (Dr. Fabio Romanelli), done in the framework of the mission at Valparaíso (November 2007), with the help of many local Organizations. The literature has been deeply and fruitfully discussed with the Chilean scientific team, in particular with Prof. R. Saragoni, Prof. M. Astroza and some of their PhD students (e.g. S. Ruiz and T. Sturn) for the Seismic Hazard and with Dr. Dante Gutierrez (SHOA) for the Tsunami Hazard.**

- Acevedo, P., Astroza, M., Canales, J.C., Monge, J., and Perretta, C., 1989. Relación entre las unidades geotécnicas y los daños producidos por el sismo del 3 de marzo de 1985 en la ciudad de Valparaíso. 5as Jornadas Chilenas de Sismología e Ingeniería Antisísmica, Santiago, Chile.
- Astroza M. y J. Monge, 1994, “Aumento de intensidades según las características geológicas de los suelos de fundación, sismo del 3 de Marzo de 1985”, Anales de la Universidad de Chile, 5a serie, No. 21, pp 103-121.
- Astroza, M., Norambuena, A., Astroza, R., 2006. Reinterpretación de las intensidades del terremoto de 1906, International Conference Montessus de Ballore 1906 Valparaíso Earthquake Centennial.
- Barrientos, S. E., 1988. Slip distribution of the 1985 central Chile earthquake, Tectonophysics 145, 225-241.
- Beresnev, I. A., and Atkinson, G. M., 1997. □ Modeling finite-fault radiation from the omega<sup>n</sup> spectrum □ Bulletin of the Seismological Society of America, 87(1):67-84.
- Caravajal, A., 1989. Estudio comparativo de los terremotos de Valparaíso de 1906 y 3 de marzo de 1985. Civil Engineer Thesis. Dept. Civil Engr. Fac. Ciencias Físicas y Matemáticas, Universidad de Chile, Santiago, Chile.
- Celebi, M., 1988. Processed Chile earthquake records of 3 March 1985 and aftershocks, U.S. Geol. Surv., Open-File Rep, 87-195, revised October 1988.
- Choy, G. L. and J. W. Dewey (1988). Rupture process of an extended earthquake sequence: teleseismic analysis of the Chilean earthquake of March 3, 1985, J. Geophys. Res. 93, 1103-1118.
- Comte, D., Eisenberg, A., Lorca, E., Pardo, M., Ponce, L., Saragoni, R., Singh, S. K., and Suárez, G., 1986. The 1985 central Chile earthquake: A repeat of previous great earthquakes in the region?. Science, 233, 393-500.
- Espinoza, P., 2000. Amplificación sísmica en suelos Y microzonificación de los sectores planas de Vina del Mar y Valparaíso, Civil Engineer Thesis. Departamento de Obras Civiles, Universidad Técnica Federico Santa María, Valparaíso, Chile.
- Lomnitz, C., 1962. On Andean structure. J. Geophys. Res. 67 1 (1962), pp. 351–363.
- Lomnitz, C., 1964. On Andean structure, part II: Earthquake risk in Chile. BSSA, 54, 1271-1281.
- Lomnitz, C., 1970. Major earthquake and tsunami in Chile during the period 1535 to 1953. Geolog. Rundschau., 59, 938-960.
- Lomnitz, C., 1983. On the Epicenter of the Great Santiago Earthquake of 1647. Bull. Seism. Soc. Am., 73, 885-886.
- Mendoza, C., Hartzell, S., and Monfret T., 1994. □ Wide-band analysis of the 3 March 1985 Central Chile earthquake; overall source process and rupture history □ Bulletin of the Seismological Society of America, 84(2):269-283
- Montessus de Ballore F., 1915, “Historia Sísmica de Los Andes Meridionales al sur del paralelo XVI, Quinta Parte: El Terremoto del 16 de agosto de 1906”. Sociedad Imprenta- Litografía Barcelona, Santiago-Valparaíso, Chile, 407 pp.
- Nishenko, S. P., 1985. Seismic potential for large and great interplate earthquake along the Chilean and Southern Peruvian margins of South America: A quantitative reappraisal. Journ. of Geophysical Research, 90, 3589-3615.
- Okal, E. A., 2005. A re-evaluation of the great Aleutian and Chilean earthquakes of 1906 August

17. *Geophys J. Int.*, 161, 268-282.
- Saragoni, R., M. Fresard, and P. Gonzales (1985). Análisis de los acelerogramas del terremoto del 3 de Marzo de 1985: Universidad de Chile, Departamento de Ingeniería Civil, Publication SES 14/1985(199).
- Saragoni, R., 2006. Estudio comparativo de los efectos de los terremotos de Valparaíso de 1906 y 1985 en el barrio El Almendral. International Conference Montessus de Ballore 1906 Valparaíso Earthquake Centennial.
- SHOA, 1999. Carta de Inundación por Tsunami para la bahía de Valparaíso, Chile. <http://www.shoa.cl/servicios/citsu/citsu.php>
- SHOA, 2003. Carta de Inundación por Tsunami - Porto-Quintero. <http://www.shoa.cl/servicios/citsu/citsu.php>
- Somerville, P. G., M. K. Sen, and B. P. Cohee, 1991, Simulation of strong ground motions recorded during the 1985 Michoacan, Mexico and Valparaiso, Chile earthquakes, *Bull. Seism. Soc. Am.*, 81(1), 1-28.
- Tanner, J.G., Shedlock, K.M., 2004, Seismic hazard maps of Mexico, the Caribbean, and Central and South America, *Tectonophysics*, 390, pp. 159– 175.
- Verdugo, A. I., 1995. Estudio geofísico de los suelos de fundación para una zonificación sísmica de Valparaíso y Vina del Mar, Civil Engineer Thesis. Dept. Civil Engr. Fac. Ciencias Físicas y Matemáticas, Universidad de Chile, Santiago, Chile.
- Verdugo, A., 2006. Amplificación sísmica en los sectores planos de Viña del Mar y Valparaíso, International Conference Montessus de Ballore 1906 Valparaíso Earthquake Centennial.
- Verdugo, R., 2006. Caracterización geotécnica de Valparaíso y su efecto en el Terremoto de 1906., International Conference Montessus de Ballore 1906 Valparaíso Earthquake Centennial.

## 9. REFERENCES

- Cancani, A., 1904. Sur l'emploi d'une double échelle sismique des intensités, empirique et absolue, *G. Beitr.* 2, 281-283.
- Cornell, C.A. (1968). "Engineering seismic risk analysis," *Bull. Seism. Soc. Am.*, 58, 1583-1606.
- Dolce, M., Martelli, A., Panza, G.F., 2005. *Proteggersi dal terremoto: le moderne tecnologie e metodologie e la nuova normativa sismica*. Seconda edizione. 21mo Secolo, 336 pagine, ISBN 88-87731-28-4.
- Fäh D., Panza G.F. (1994). "Realistic modelling of observed seismic motion in complex sedimentary basins", *Annali di Geofisica*, 37, 1771-1797.
- GSHAP. The Global Seismic Hazard Assessment Program. <http://seismo.ethz.ch/gshap/index.html>
- Gusev, A.A., 1983. Descriptive statistical model of earthquake source radiation and its application to an estimation of short period strong motion. *Geophysical Journal of the Royal Astronomical Society* 74, 787–800.
- Gusev, A.A., Pavlov, V., 2006. Wideband simulation of earthquake ground motion by a spectrum-matching, multiple-pulse technique. First European Conference on Earthquake Engineering and Seismology (a joint event of the 13th ECEE & 30th General Assembly of the ESC). Geneva, Switzerland, 3–8 September 2006. Paper Number: 408.
- Haskell, N., 1964. Total energy and energy spectral density of elastic wave radiation from propagating faults. *Bulletin of the Seismological Society of America* 56, 1811–1842.
- Klügel, J.-U., 2007. Error inflation in probabilistic seismic hazard analysis. *Engineering Geology* 90, 186–192.
- Panza, G.F., Suhadolc, P. (1987). "Complete strong motion synthetics", In: *Seismic Strong Motion Synthetics, Computational Techniques* 4, B.A. Bolt (Editor), Academic Press, Orlando, 153-204.



- Panza, G.F., Suhadolc, P. (1989). "Realistic simulation and prediction of strong ground motion", In: Computers and experiments in Stress Analysis, G.M. Carlomagno and C.A. Brebbia (Editors), Springer-Verlag, 77-98.
- Panza, G.F., Vaccari, F., Costa, G., Suhadolc, P., Fäh, D. (1996). "Seismic input modelling for Zoning and microzoning", *Earthquake Spectra*, 12, 529-566.
- Panza, G. F., Vaccari, F. and Cazzaro, R., 1997. Correlation between macroseismic Intensities and seismic ground motion parameters, *Ann. Geof.*, 15, 1371-1382.
- Panza, G.F., Vaccari, F. And Romanelli, F, 1999. The IUGS-UNESCO IGCP Project 414 : Realistic Modeling of Seismic Input for Megacities and Large Urban Areas. *Episodes*, March 1999, Vol.22, No.1, p. 26-32.
- Panza, G.F., Romanelli, F., Vaccari, F., 2000. "Realistic modelling of waveforms in laterally heterogeneous anelastic media by modal summation", *Geophys. J. Int.*, 143, 1-20.
- Panza, G.F., Romanelli, F., Vaccari, F., 2001. "Seismic wave propagation in laterally heterogeneous anelastic media: theory and applications to the seismic zonation", *Advances in Geophysics*, Academic press, 43, 1-95.
- Panza, G.F., Romanelli, F., Vaccari, F., Decanini, L., Mollaioli, F., 2003. "Seismic hazard evaluation in South-Central Europe and Mediterranean region: state of the art", this issue.
- Parvez, I. A., Vaccari, F., Panza, G. F., 2003. A deterministic seismic hazard map of India and adjacent areas. *Geophysical journal international* , 2003, Vol. 155, n. 2, pp. 489-508.
- Peresan, A., Kossobokov, V., Romashkova, L., Panza, G.F., 2005. Intermediate-term middle-range earthquake predictions in Italy: a review. *Earth-Science Reviews* 69 2005 97-132.
- Romanelli, F., Vaccari, F. (1999). "Site response estimation and ground motion spectral scenario in the Catania Area", *J. of Seism.*, 3, 311-326.
- Romanelli, F., Vaccari F., Panza, G.F. (2001). "Application of the modal summation technique to the theoretical site response estimation", *Journal of Computational Acoustics*, 9, 643-653.
- Romanelli, F., Vaccari, F. and Panza, G.F., 2003. Realistic Modelling of the Seismic Input: Site Effects and Parametric Studies, *Journal of Seismology and Earthquake Engineering*, Vol. 5, No. 3, pp. 27-39.
- Romanelli, F., Panza, G.F. and Vaccari, F., 2004. Realistic Modelling of the Effects of Asynchronous motion at the Base of Bridge Piers, *Journal of Seismology and Earthquake Engineering*, Vol. 6, No. 2, pp. 19-28.
- Senior Seismic Hazard Analysis Committee (SSHAC), 1997. Recommendations for probabilistic seismic hazard analysis: guidance on uncertainty and use of experts. NUREG/CR-6372.
- Vaccari, F., Romanelli, F., Panza, G.F., 2005. Detailed modelling of strong ground motion in Trieste. *GT&A* 2, 7-40.
- Zuccolo, E., et al., 2008. Neo-deterministic definition of seismic input for residential seismically isolated buildings, *Engineering Geology* (2008), doi:10.1016/j.enggeo.2008.04.006
- Wessel, P., and Smith, W.H.F., 1991. Free software helps map and display data, *EOS Trans. AGU*, 72, 441.